EAEME Course on
Risk Assessment & Control of Major Accident Hazards

Models for Description of Accident Consequences

G. Spadoni
Dept. of Chemical and Process Engineering
University of Bologna - Italy

INTRODUCTION

The aim of this short report is to introduce and explain the main concepts at the basis of the models most widely used to assess the physical consequences of accidents in chemical plants, and in storage or transport of dangerous substances.

The scientific literature suggests a large number of simplified and detailed physical models, which can be classified in the following four categories:

- **source term models**
  to provide quantitative information on source rates of liquids and gas/vapours
- **fire models**
  to estimate thermal flux due to flammable releases
- **explosion models**
  to calculate overpressures resulting from the ignition of flammable clouds
- **dispersion models**
  to predict the atmospheric dispersion of vapours by evaluating their concentrations in air.

Threshold values for heat radiation, overpressure and concentration are often utilised to evaluate the safety distances for people and structures (buildings, apparatuses, plants), but the best way to estimate damages due to physical impacts is to adopt **vulnerability models**, or effect models, as they can predict the spatial distribution of the probability of the reference damage.

The models included in the categories above cited represent the basic tools of a **consequence analysis**, whose uses are manifold and more precisely:

- *in the design of a plant*, to make clear the need of protection and prevention measures and to design specific mitigation systems ;
- *in the risk analysis of a plant*, to establish the goodness of the adopted safety measures;
- *in the risk analysis of an industrial area*, to help in assessing the impact of several industrial plants, with the related transports (by road, by train, by ship, by pipelines), on a densely populated area.

The models able to fulfil these aims can require different levels of detail: as an example the optimal design of a bund calls for a mathematical description of the evaporation phenomenon which is surely more precise than that required to estimate a mean evaporative rate; therefore, depending on the required goal, a simplified model too can assure good results, even if the use of detailed models must generally be preferred.

In this report the attention is mainly focused on simplified and intermediate models widely used for plant and area risk analysis; only some hints and many references are given to cover the field of detailed models. Moreover , for sake of shortness, only an introduction is given to source models; after all most of them

derive from methods usually adopted in design and analysis of chemical plants and does not provide a deeper knowledge of risk analysis.

1. SOURCE MODELS AND ACCIDENT OUTCOMES

Most accidents result in spills of toxic, flammable and explosive materials. For example, material is released from holes and cracks in tanks and pipes, from leaks in flanges, pumps, and valves, and a large variety of other sources.

The event tree of Fig.1-1 shows all potential incident outcomes from the release

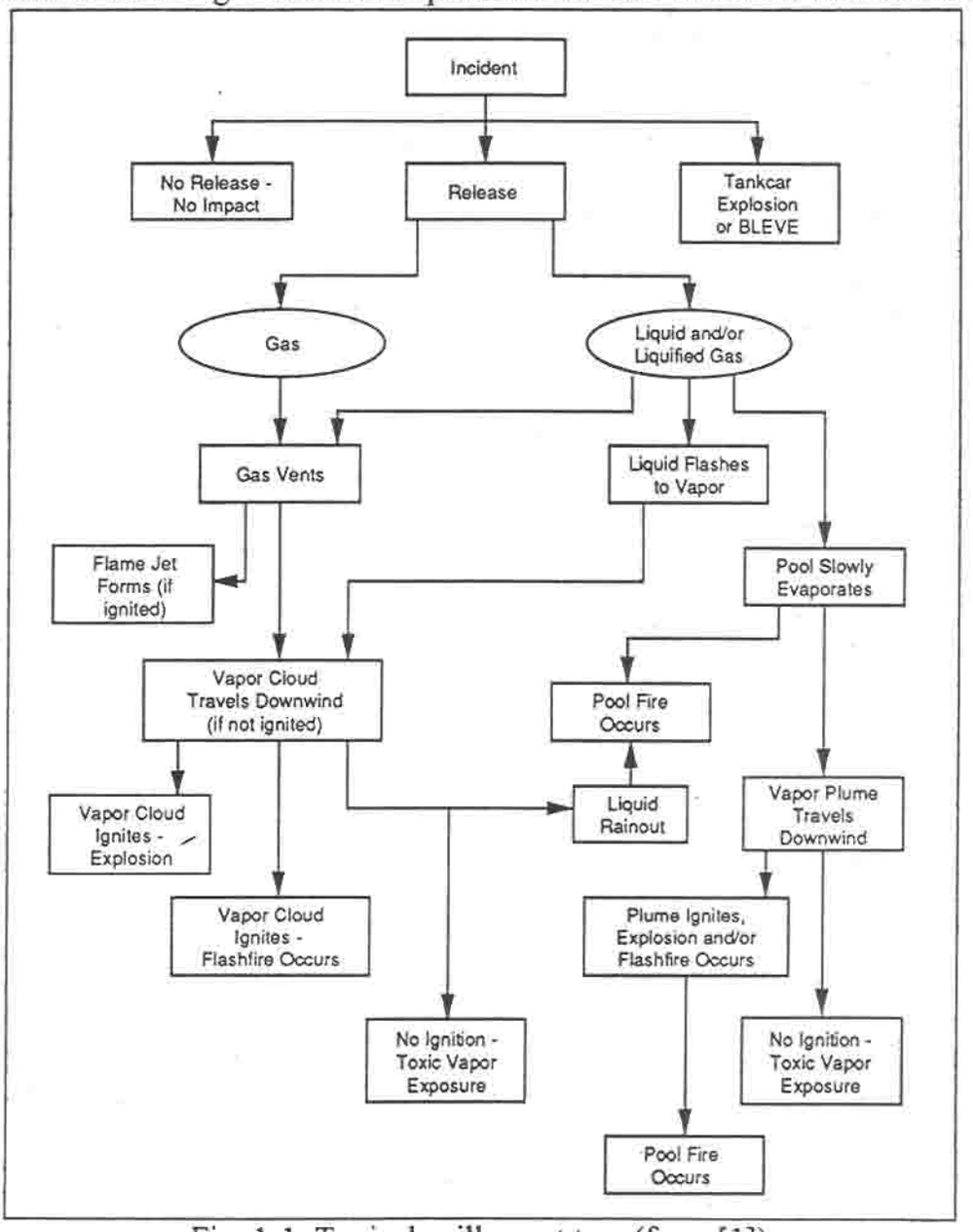

Fig. 1-1. Typical spill event tree (from [1])

(loss of containment) of a hazardous chemical. Naturally, the properties of the chemical, conditions of the release, etc., all influence which of the logical path

will apply for any specific accident evolution.

Some blocks address three different types of sources: a jet of gas or vapour, a stream of liquid or a stream of flashing liquid, when this is stored under pressure above its atmospheric boiling point.
The ambient evolution of a liquid leads to an evaporative pool to be formed, while flashing liquid gives partially rise to vapour, which might also transport small liquid droplets or aerosols.

Source models are used to quantitatively define the release by estimating discharge rates, and extent of flash and evaporation from a liquid pool.
The basic source models, which are used repeatedly, are

1. flow of liquid through a hole in a tank
2. flow of liquids through pipes
3. flow of vapour through a hole in a tank
4. flow of vapour through pipes
5. flashing liquids (and two-phase flows)
6. liquid pool evaporation or boiling.

The underlying technology for models from 1 to 4 is well developed in chemical engineering theory and full descriptions are available in standard references [2,3]. Greater care must be devoted to the treatment of two-phase discharge, flashing liquid and evaporation from a pool, the modelling of which is frequently more empirical.

A superheated liquid flowing from a pipe breakage begins to vaporise into the pipe and a two-phase flow results; semi-empirical methods to evaluate its flow rate can be found in [4,5,6,7]. In any case the liquid will flash when released to the atmosphere: aerosol entrainment in the vapour produced and/or the rainout onto the ground have very significant effects on cloud dispersion and, above all, contribute to an higher density of the cloud.

The fraction of released liquid vaporised F_v can be estimated in a number of ways; the standard equation for flash prediction of a pure substance is

$$F_v = c_p \frac{(T - T_b)}{h_{fg}} \qquad (1.1)$$

where

c_p = heat capacity of liquid (averaged over T to T_b) (kJ/kg K)
T = initial temperature of liquid (K)
T_b = atmospheric boiling point of liquid (K)
h_{fg} = latent heat of vaporisation of liquid at T_b (kJ/kg)

F_V is a poor prediction of the total mass of material in the vapour cloud because of the possible presence of entrained liquid as droplets. On the basis of historical accidents and experiments, some authors [8] proposed **entrained liquid fraction** (F_L) to be evaluated through the following criteria:

- $F_L = 1 - F_V$ if $F_V > 30\%$ (liquid is completely entrained as droplets),
- $F_L = F_V$ if $15\% \leq F_V \leq 30\ \%$, and the remaining liquid forms a pool

- $F_L = 0.$ if $F_V \leq 15\%$: the liquid forms a pool.

A detailed physical mathematical model for a vapour jet with aerosol entrainment is proposed in [9].

Evaporation from liquid spills onto land and water has received substantial attention. Land spills can occur into a dike or other retention system that allows the pool size to be better estimated; when spills are unbounded calculations are more complex and partly empirical. A complete review of pool evaporation modelling is presented in [10]; numerical codes are also available [11,12]. Models distinguish in general evaporation of high-boiling liquids from vaporisation of low-boiling (cryogenic) liquids. Diffusional mechanism, solar heat flux and convective heat transfer from atmosphere govern the former phenomenon while heat transfer from ground controls the latter, at least in the initial stage.

The spill event tree of Fig. 1-1 introduces accidental outcomes, and their modelling is necessary when physical consequences must be evaluated. Looking at the figure, the following outcomes result:

BLEVE

a **B**oiling **L**iquid **E**xpanding **V**apour **E**xplosion occurs from the sudden release of a large mass of pressurised liquid to the atmosphere (primary causes are: an external flame impinging on the shell of a vessel above the liquid level, weakening the shell and resulting in a sudden rupture; an external fire embracing the vessel). When ignited the vapour give rise to a FIREBALL

FIREBALL

the atmospheric burning of a fuel-air cloud in which the energy is mostly emitted in the form of radiant heat. The inner core of the fuel released consists of almost pure fuel whereas the outer layer is a flammable fuel-air mixture. As buoyancy forces of the hot gases begin to dominate, the burning cloud rises and becomes more spherical in shape

POOL FIRE

the combustion of material evaporating from a layer of liquid at the base of the fire

JET FIRE

fire type resulting from fires from pressurised release of gas and/or liquid

FLASH FIRE

the combustion of a flammable vapour and air mixture in which flame passes through that mixture at less than sonic velocity, such that negligible damaging overpressure is generated

UNCONFINED **V**APOUR **C**LOUD **E**XPLOSION (UVCE)

when a flammable vapour is released, its mixture with air will form a flammable vapour cloud. If ignited, the flame speed may increase to high velocities and

produce significant blast overpressure

ATMOSPHERIC DISPERSION

the low momentum mixing of a gas or vapour with air. The mixing is the result of turbulent energy exchange which is a function of wind (mechanical eddy formation) and atmospheric temperature profile (thermal eddy formation)

2. FIRE MODELS

The objective of this section is to review the types of models available for the estimation of fire incident outcomes. The physical consequences of concern are thermal radiation fluxes. The section contains the following subsections:

- pool fires and jet fires
- BLEVE and fireball

2.1 Pool fires and jet fires

2.1.1 Pool Fire

The pool fire is a common fire type resulting from a fire over a pool of liquid. It tends to be localised in effect, especially in chemical plants where often releases of flammable substance are confined in bunds, and is mainly of concern in establishing the potential for domino effects and employee safety zones. The effects can be of greater importance when the release occurs on a unconfined ground, as it can happen for accidents in transport by road, rail or pipeline.

Pool fire modelling is well developed, detailed reviews and suggested formulas are provided in [1,10].

The received thermal flux from a pool fire is determined by

$$Q(x) = \tau E F_a \qquad (2.1)$$

where

$Q(x)$ = thermal radiation received at distance x (kW/m^2)

τ = atmospheric trasmissivity (fraction of energy transmitted: 0 to 1, dimensionless)

E = surface emitted flux per unit area (kW/m^2)

F_a = geometric view factor, flame surface to target (dimensionless)

(Where human injury is being considered, it may be necessary to add solar radiation to account for total radiation received.)

With reference to the eqn. 2.1, it is worth noting that the coefficient τ is dependent both on the characteristics of the atmosphere (relative humidity, temperature and composition) and the distance of the receiving object, the emitted power depends on burning substance and the geometric view factor is

affected by pool size and flame height.

Pool size and flame height

In most cases, pool size is fixed by the size of the release and by local physical barriers (dikes,..). Circular pool are normally assumed; where dikes lead to square or rectangular shapes an equivalent diameter is used.

Let be D the diameter of the pool and H the visible flame height; H can be related to D by using experimental observations. The best known correlation is [13]

$$\frac{H}{D} = 42\left[\frac{m_b}{(\rho_a \sqrt{gD})}\right]^{0.61} \qquad (2.2)$$

where

m_b = burning rate (kg/m^2 s)
ρ_a = ambient air density ($\cong$1.2 kg/ m^3)
g = acceleration of gravity (9.81 m/s^2)

Experiments have shown that large pool fires burn at constant vertical rate, characteristic for the material. Typical values for hydrocarbons are in the range 0.05(gasoline) ÷ 0.12 (LPG) [14].

The most widely used correlation is [10]

$$m_b = 10^{-3} K \frac{h_c}{h_v (T_\infty)} \qquad (2.3)$$

where

h_c = heat of combustion (kcal/ kg)
h_v = heat of vaporisation (kcal/ kg)
T_a = ambient temperature
K = $h_v / (h_v + c_p (T_b - T_a))$, *when* $T_b > T_a$, *otherwise* $K = 1$.

The knowledge of the burning rate permits an equivalent diameter to be computed when a *continuous release* is considered. In fact, for a release on a flat plane the maximum diameter of the pool, which is reached when the product of burning rate and surface area equals the release rate, is assumed.

Surface emitted power

It can be computed from the Stefan-Boltzmann equation, which is very sensitive to the assumed flame temperature, as radiation varies with temperature to the fourth power. Further, the obscuring effect of smoke substantially reduces the

total emitted radiation. An alternative approach uses an experimental correlation [10] which includes smoke absorption of radiated energy

$$E = \frac{0.35 \times m_b \times h_c}{1 + 168\left[\frac{m_b}{\rho_a \sqrt{g}}\right]^{0.61}}$$

Tab 2.1 gives values of surface emitted powers for some low-boiling and high-boiling liquids.

Substances with $T_b < 20°C$	E (kW/m^2)	Substances with $T_b > 20°C$	E (kW/m^2)
Ammonia	17	Acetone	42
Butane	86	Acetonitrile	34
Butadiene	87	Acrylonitrile	36
1-Butane	87	Allyl Alcohol	37
Dimethylamine	59	Benzene	71
Ethane	96	Diethylamine	71
Ethylchloride	28	Ethylene Diamine	36
Ethylene oxide	37	Ethyl Formate	29
Carbon monoxide	13	Ethyl Mercaptane	45
Methane	100	Hexane	87
Methyl bromide	9	Methanol	19
Methyl chloride	15	Methyl Acetate	26
Propane	98	Methyl Formate	18
Propylene	92	Vinyl Acetate	32
Vinylchloride	26	Carbon Disulphide	15
Hydrogen sulphide	18		

Table 2-1 Radiation emittance (E) of the flame surface of boiling ($T_b<20°C$) and non-boiling ($T_b>20°C$) pools

Geometric view factor

This factor is the ratio of emitted power (ignoring atmospheric absorption) received by the target. View factors for different emitting and receiving surfaces are discussed in texts on thermal radiation [15].

If we consider a cylindrical flame, vertically oriented, and a receiving surface the dimensions of which are negligible in comparison with the flame, the following table (Tab. 2-2) can be used to determine F_a values.

In this table x is the distance of the receiving object from the centre of the pool. As the view factor depends on both emitting and receiving objects, two sections are presented, respectively for vertical and horizontal targets.
Pool fires are often tilted by the wind [16] and this effect alters the radiation received at surroundings locations, as a consequence the flame does not radiate equally in all directions as it happens for vertical flames. Numerical difficulties

arise in view factor evaluations for different directions (downwind or upwind). Moreover a complete QRA would require computations in several wind directions [10].

2H/D	0.1	0.2	0.5	1.0	2.0	3.0	5.0	6.0	10.0	20.0
2x/D		1) horizontal plane (10^3 F_h)								
1.1	132	242	332	354	360	362	362	362	363	363
1.2	44	120	243	291	307	310	312	312	313	314
1.3	20	665	178	242	268	274	277	278	278	279
1.4	11	38	130	203	238	246	250	251	252	253
1.5	6	24	97	170	212	222	228	229	231	232
2.0	1	5	27	73	126	145	158	160	164	166
3.0			5	19	50	71	91	95	103	107
4.0			1	7	22	38	57	62	73	78
5.0				3	11	21	37	43	54	61
10.0					1	3	7	9	17	26
20.0							1	1	3	8
	2) vertical plane (10^3 F_v)									
1.1	330	415	449	453	454	454	454	454	454	455
1.2	196	308	397	413	416	416	416	416	416	417
1.3	130	227	344	376	383	384	384	384	384	385
1.4	94	173	296	342	354	356	356	357	357	357
1.5	71	135	253	312	329	332	333	333	333	333
2.0	28	56	126	194	236	245	248	249	249	250
3.0	9	19	47	86	132	150	161	163	165	167
4.0	5	10	24	47	80	100	115	119	123	125
5.0	3	6	15	29	53	69	86	91	97	100
10.0		1	3	6	13	19	29	32	42	48
20.0				1	3	4	7	9	14	21

Tab. 2-2 view factors for a vertical cylindrical flame

Atmospheric trasmissivity

A significant part of the heat flux emitted by the flame can be absorbed or scattered by the atmosphere (over 20% for distances greater than 20 m). The following correlation, which accounts for air humidity, is recommended [17]

$$\tau = 2.02 \left(P_w X\right)^{-0.09} \qquad (2.4)$$

where

τ = atmospheric trasmissivity (fraction of energy transmitted: 0 to 1)
P_w = partial pressure of water (Pa)
X = path length, distance from flame surface to target (m)

2.1.2 Jet fire

Jet fires result from pressurised releases of gas and/or liquid. They are localised and assume a special importance in assessing the potential for domino effects on adjacent hazardous vessels, because the dimensions of the jet flame can be used to determine whether flame impingement occurs. Jet fire modelling is not as well developed as for pool fires, but several reviews have been published [18,19,20].

The best known method considers the fire dart as a cylinder and evaluates heat radiation by adopting eqn. 2.1. Of course complex numerical computations are required for the evaluation of view factors, owing to the wide variety of directions and heights a jet can have. Empirical correlations allow the length L and diameter D of the jet to be calculated for a turbulent flow respectively from [21,22]

$$\frac{L}{d} = \frac{5.3}{c_t}\left\{\frac{T_{fl}}{\alpha_t T_n}\left(c_t + (1-c_t)\frac{M_a}{M_s}\right)\right\}^{\frac{1}{2}} \qquad (2.5)$$

where

d = diameter of flow section (m)
M_a = molecular weight of air (kg/kmol)
M_s = molecular weight of flammable substance (kg/kmol)
T_{fl} = flame temperature (K)
T_n = gas initial temperature (K)
c_t = molar fraction of the gas in the stoichiometric air-fuel mixture
α_t = ratio between moles of reactant and combustion product (stoichiometric reaction)

$$D = 0.29x\left(\ln\frac{L}{x}\right)^{\frac{1}{2}} \qquad D_{max} = 0.12L \quad \text{at} \quad x = 0.61L \qquad (2.6)$$

where x is the distance along the jet axis.

≈≈≈≈≈≈≈≈≈≈≈≈≈≈≈

2.1.3 Sample problem

N.1

Determine the thermal flux received at a distance of 100 m from a pool fire of Hexane in a 25-m diameter tank dike. Weather conditions are no wind, 20 °C and 50% relative humidity. Assume a burning rate = 0.13 kg /m^{2}s.

$$\tau = 2.02\,(P_w\ X)^{-0.09} = 2.02(2320 \times 100)^{-0.09} = 0.66$$

Flame height (eqn. 2.2)

Flame height (eqn. 2.2)

$$\frac{H}{D} = 42\left[\frac{m_b}{\left(\rho_a\sqrt{gD}\right)}\right]^{0.61} = 42\left(\frac{0.13}{\left(1.2\sqrt{9.81\times 25}\right)}\right)^{0.61} = 2.02 \longrightarrow H = 50.5\ m$$

As the view factor for a receiving vertical surface (tab.2-2) F_a is 0.045 and E is 87 kW/m^2 (tab. 2-1), the received thermal flux results 2.6 kW/m^2.

2.2 BLEVE and Fireball

The phenomenon of BLEVE was described in a previous section. It results in a sudden failure of containment allowing a superheated liquid to flash. The increase in volume is sufficient to generate a pressure wave and fragments and if the released liquid is flammable a **fireball** may occur.

The best known type of BLEVE involves LPG. A number of such incidents have occurred including San Carlos, Spain (1978) and Mexico City, Mexico (1984).

The modelling philosophy is primarily empirically based [23,24,25] and includes pressure, fragments and heat radiation effects.

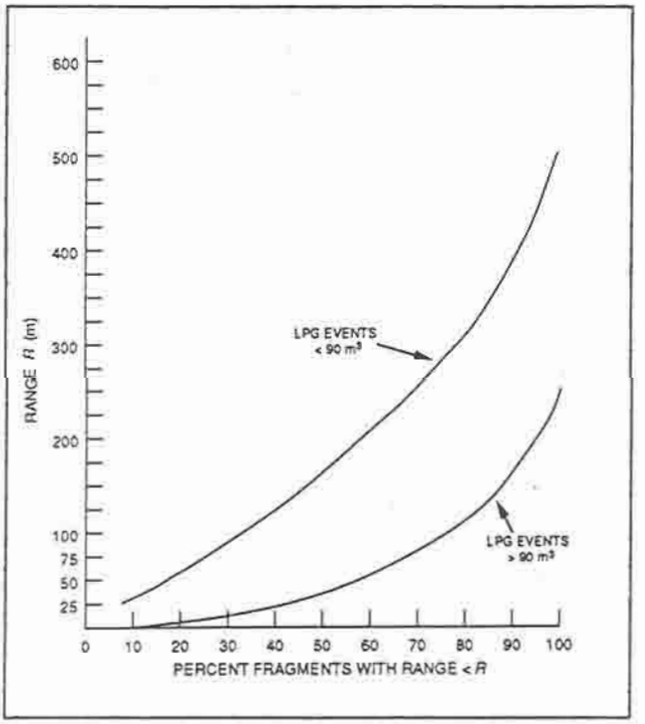

Fig. 2-1 Fragment range in LPG events.

Pressure effects are usually limited in magnitude and are thus of interest primarily for the prediction of domino effects on adjacent vessels rather than for harm to neighbouring communities.

The prediction of **fragment effects** is important, as fragments can cause many deaths and domino damage effects. Specific works on BLEVE fragmentation hazards can be found in [26]. In [27] graphs are reported showing fragment ranges.

The Fig. 2-1 shows that about 80% of fragments fall within a 300 m range.

The total number of fragments (N) is a function of the vessel capacity (V): the following correlation, based on seven incidents, was proposed

$N = -3.77 + .0096\ (\ V\ (m^3))$

(range of validity 700-2500 m^3)

Heat radiation effects can be computed once dimensions and duration of the fireball have been established. All proposed models [17,24] use power law correlations based on observed data; the most useful formulas are

Peak fireball diameter (m)	D_{max}	$= 6.48\ M^{0.325}$
Fireball duration (s)	t_{bleve}	$= 0.825\ M^{0.26}$
Centre height of fireball (m)	H	$= 0.75\ D_{max}$

where M = initial mass of flammable liquid (kg).

Referring to Fig. 2-2, the radiation received by a target is given by

$$Q(x) = \tau\, E\, F_f \qquad (2.7)$$

where

Q(x) = thermal radiation received by a black body target (kW/m^2)

τ = atmospheric trasmissivity (dimensionless)

E = surface emitted flux per unit area (kW/m^2)

F_f = geometric view factor (dimensionless)

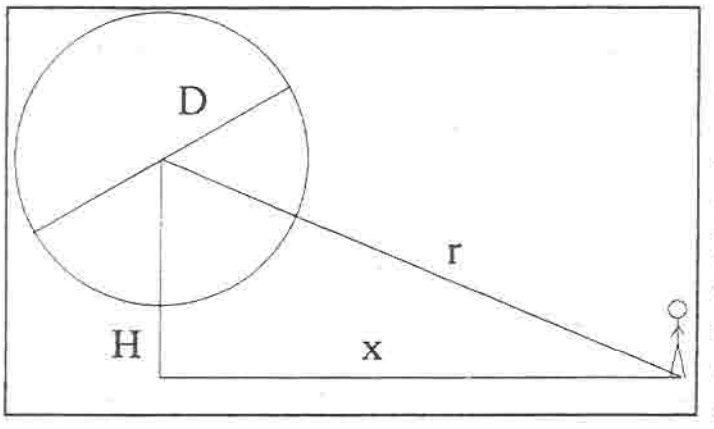

Fig. 2-2 schematic drawing of a fireball

The methods to calculate E and F_f are different from those used for pool fires.

Surface emitted power

Typical heat fluxes in BLEVE (200-300 kW/m^2) are much higher than in pool fires as the flame is not smoky. The following formula is proposed in [28]

$$E = \frac{F_{rad}\, M\, H_c}{\pi\,(D_{max})^2\, t_{Bleve}} \qquad (2.8)$$

where

M = mass of LPG in BLEVE (kg)

H_c = heat of combustion (kJ/kg)

F_{rad} = radiation fraction, typically .25-.40

To evaluate the geometric view factor between a sphere and a target point we use

$$F_f = \frac{D^2}{4r^2} \qquad (2.9)$$

where r is the distance from the sphere centre to the target (m).

Once the radiation received is calculated the human harm can be determined from vulnerability models (see Sec. 5).

2.2.1 Sample problem

N.1

Calculate the size and duration, and thermal fluxes at distances from 100 to 1000 m for a BLEVE of an isolated 10^5 kg tank of propane at 20 °C, 8.2 bar. Atmospheric humidity corresponds to a water partial pressure of 2810 Pa.

D_{max}	$= 6.48\ (100000)^{0.325}$	= 273 m
t_{bleve}	$= 0.825(100000)^{0.26}$	= 16.5 s
H	$= 0.75\ D_{max}$	= 204 m

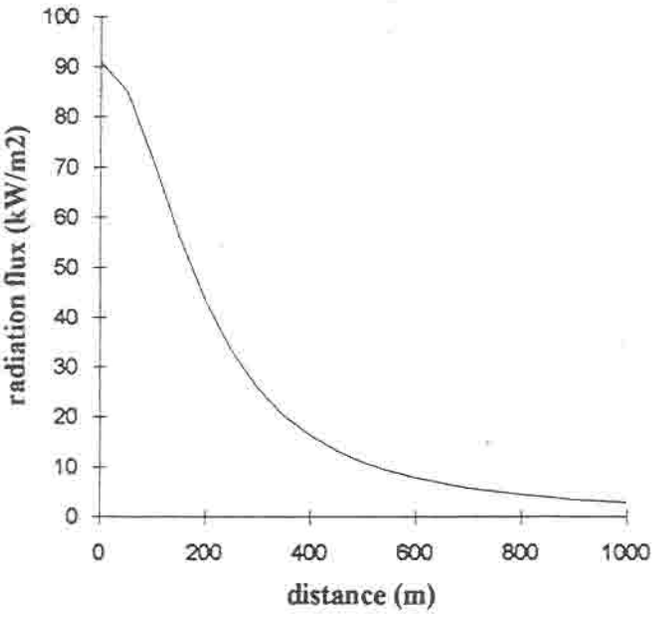

Surface emitted flux (eqn. 2.8) is 300 kW/m^2 . Heat radiation fluxes at different distances are plotted in Fig. 2.3.

Fig. 2.3 Radiation flux versus distance.

3. EXPLOSION MODELS

In this section the attention will be devoted to the models available for the estimation of accidental explosion outcomes.

Strictly speaking the locution *explosion* means a very rapid exothermic oxidation (combustion) of an ignited fuel, so that the expansion of gases results in a rapidly moving pressure or shock wave. Therefore no observation will be done on *physical explosion models* which describe the bursting of pressurised vessels: suggestions for modelling bursting are reported in [29,10].

The consequences of concern in studies for explosions are in general shock wave overpressure effects and projectile effects, while the thermal radiation effects are ignored because the shock wave effects will predominate.

Two types of explosions are possible: *deflagration or detonation.* Deflagration occurs when the overpressure wave is moving at a speed less than the speed of sound (300 m/s) in the unreacted medium, while detonation is governed by a shock wave speed greater than sound speed (up to 2 km/s). Transition from deflagration to detonation can occur in pipelines.

Moreover accidental explosions can be *confined or unconfined.*

Confined explosions include deflagrations which are constrained within vessels and buildings. Examples of these are dust or vapour explosions within low strength containers and thermal decomposition or runaway reactions within process vessels and equipment. Vessels can be designed to contain internal deflagrations. The design of relief systems for both low strength enclosures and process vessels is covered in [30]. When the peak pressure is sufficient to cause vessel or building failure the consequences can be determined by using the simple TNT model [31,32].

An **unconfined explosion** is usually the result of flammable vapour spill. The gas is dispersed and mixed with air and if the cloud is ignited before it is diluted below its LFL (Lower Flammability Limit) an **UVCE** (Unconfined Vapour Cloud Explosion) will occur. UVCE incidents are likely in process plants and transportation.

3.1 Preliminary observations on UVCEs

The combustion processes of large vapour clouds are not completely understood: a review of the historical records indicates the release of a small quantity of vapour is likely to result in **flash fire** without significant overpressure.

On the basis of the study of incidents various authors have concluded that

- there may be some minimum mass of flammable material that is required to allow transition from a flash fire to UVCE (from 1 t [33] to 15 t [34]), but

some caution should be exercised in a determination of a minimum value (examples are known of quantities as low as 100 kg for hydrogen or acetylene)

- the presence of some confinement/obstacles may be necessary for transition to UVCE
- materials with higher fundamental burning velocities can produce easier transition to UVCE for a given release quantity
- UVCE should be considered as deflagrations, not detonations
- peak overpressures of UVCEs are much less than those of detonations, typically 1 bar or less and positive phase duration of 20-100 ms[1].

Flammable vapour clouds may be ignited from either continuous (pilot flames,..) or occasional sources (smoking, vehicles, electrical system) and the ignition can occur away from the release source. It is worth noting that early ignition, before the cloud becomes fully formed, might result in a flash fire or an explosion of smaller size, while late ignition could result in an explosion of a maximum possible effect.

In the following the TNT and the TNO correlation models will be presented; they allow the consequences of UVCE to be simply evaluated. Some hints are also given to estimate flash fire damages.

3.2 UVCE - TNT model

This model uses the assumption of equivalence between the flammable material and TNT, factored by an explosion yield term

$$W = \frac{\eta M E_c}{E_{c,TNT}} \qquad (3.1)$$

where

W	= equivalent mass of TNT (kg)
M	= mass of flammable material released
η	= empirical explosion yield (or efficiency) (from 0.01 to 0.1)
E_c	= lower heat of combustion of flammable gas (kJ/kg)
$E_{c,TNT}$	= heat of combustion of TNT (4500 kJ/kg)

The explosion effects of a TNT charge are well documented; peak overpressure versus scaled ground distance is plotted in Fig. 3-1. The TNT line has been corrected to account for difference between detonation and deflagration.

---

[1] At a given distance from an explosion source the pressure will increase rapidly to a maximum (peak overpressure) when the overpressure wave arrives and then will decrease up to the ambient pressure in a time-interval which is named positive phase duration.

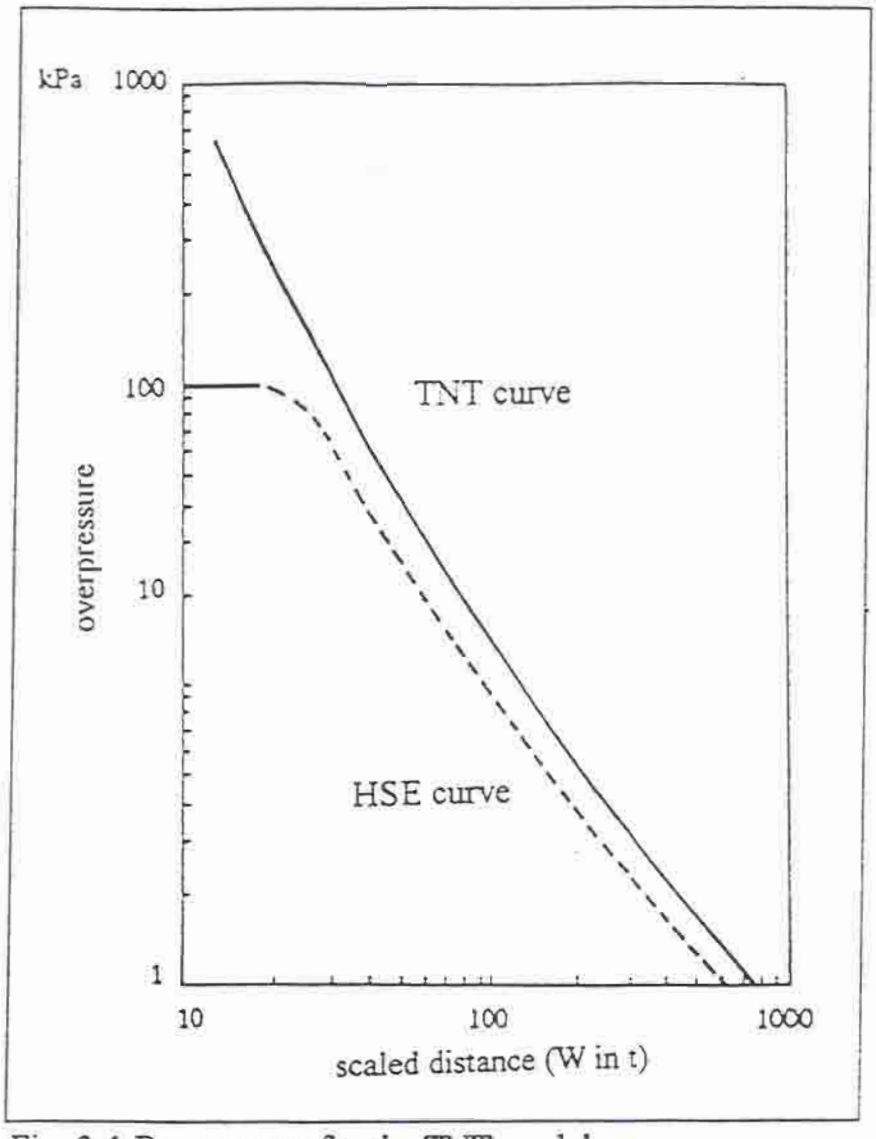

Fig. 3-1 Base curves for the TNT model

The scaled distance Z_G is given by

$$Z_G = x/W^{1/3} \quad (3.2)$$

The model is very simple, but a large error can be done in the choice of explosion yield. In fact the range 1-10% affects predicted distances by more than a factor of two. Another error may be in the estimation of the flammable cloud mass, which is based on flash, evaporation and dispersion calculations, which are also subjected to errors. Dispersion calculations are useful to determine cloud mass and extent.

3.3 UVCE - TNO model (or piston model) [10]

The gas-air mixture, assumed as an hemispherical cloud of volume V_0, expands, after ignition in the centre, to an hemisphere with volume V_1. This expanding movement is responsible for the formation of the shock wave, and in the development of the model is replaced by an equivalent piston movement. This movement can take place at different speeds.

On the basis of experiments, the peak overpressure of the blast wave has been related to the distance to the final hemispherical cloud for a number of different piston speeds. The ratio between r_1, the radius of the hemisphere of volume V_1, and the time in which the expansion takes place gives an average value of the flame velocity u_f.

The simple calculation method consists of two steps:

1. to calculate the characteristic explosion length L_0

$$L_0 = \left(\frac{V_0 \; E_c}{p_0} \right)^{1/3} \qquad (3.3)$$

where p_0 = initial pressure of the mixture and E_c = combustion energy of fuel-air mixture (for hydrocarbons-air mixtures $E_c \approx 3.5 \times 10^6$ J/m^3)

2. to estimate overpressure Δp versus distance r

$$\frac{\Delta p}{p_0} = 2 \times 10^{-2} \times \left(\frac{r}{L_0} \right)^{-1} \qquad u_f = 40 \; m/s \qquad (3.4)$$

$$\frac{\Delta p}{p_0} = 6 \times 10^{-2} \times \left(\frac{r}{L_0} \right)^{-1} \qquad u_f = 80 \; m/s \qquad (3.5)$$

$$\frac{\Delta p}{p_0} = 15 \times 10^{-2} \times \left(\frac{r}{L_0} \right)^{-1} \qquad u_f = 160 \; m/s \qquad (3.6)$$

The average value of the flame velocity, which affects the overpressure distribution in an UVCE, has been related to the "reactivity" (*susceptibility to a flame acceleration*) of a gas-air mixture. Gases have been divided into reactivity classes (low, average, high reactivity) by using data (size of explosion range, minimum ignition energy, auto-ignition temperature,..) which give useful direct and indirect information. Tab. 3-1 gives explosion limits and reactivities of some gases and liquids.

3.4 Flash fire modelling

Flash fire modelling is not well developed. A simple approach is to use an appropriate dispersion model (see sec. 4) to determine the isopleth defining the LFL or 1/2 LFL as the assumed *limit to this zone*. The use of either of these isopleths to define thermal radiation effects require the assumptions that the combustion process is not intense and is of short duration. These assumptions are not always true: they simplify the calculation process but may underestimate the area of consequences.

Gas	Explosion limits (vol. %)	Shock wave model reactivity	Liquid	Explosion limits (vol. %)	Shock wave model reactivity
Acetaldehyde	4-57	average	Acrylonitrile	3-17	average
Ammonia	15-28	low	Acetonitrile	3-?	average
1,3 Butadiene	1.1-12.5	average	Alluyl chloride	3.2-11.2	low
n-Butane	1.5-8.5	average	Carbon disulphide	1-60	high *
Propane	2.1-9.5	average	Diethylamine	1.7-10.1	average
Propene	2-11.7	average	Propylene oxide	1.9-37	high *
1-Butene	1.6-10	average	Vinyl acetate	2.6-13.4	high *
Dimethylamine	2.8-14.4	average	Tetra ethyl lead	1.8-?	low
Ethyl chloride	3.8-15.4	low	Allyl alcohol	2.5-18	high *
Ethane	3.-13.5	average	Benzene	1-8	high *
Ethene	2.7-34	average	1,3 Dichloropropene	3.5-14.5	low
Ethylene oxide	3-100	high	Epichlorhydrin	2.3-34.4	low
Methane	5-15	low	Ethylene diamine	2.7-16.6	average
Methyl bromide	8.6-20	low	Ethyl formate	2.7-13.5	high *
Methyl chloride	10.7-17.2	low	Formic acid	14-33	average
Vinyl chloride	4-29	average	Methyl acrylate	2.8-25	high *
Formaldehyde	7-73	high *	Methyl formate	5-23	high *
Carbon monoxide	12.5-74.2	low	Solvent naphtha	1.0-7.5	high *
Hydrogen sulphide	4.3-46	high *	Ethyl mercaptan	2.8-18.2	high *
Acetylene	1.5-100	high	t-Butyl mercaptan	?	high *
			n-Butyl mercaptan	?	high *
			Tetrahydrotiophene	?	high *

Tab. 3-1 Explosion limits and reactivities of various gases and liquids (* indicates poor information)

3.5 Sample problem

N. 1

Use TNT and TNO models to calculate the distance to 0.1 bar overpressure (equivalent to repairable building damages).

Data: Propane (average reactivity), M = 10 t; E = 46350 kJ/kg; $\eta = 0.05$

With TNT model

$$W = \frac{.05 \times 10000 \times 46350}{4500} = 5150 \text{ kg}$$

From Fig. 3.1 the scaled distance to 0.1 bar is about 55 $m/t^{1/3}$ for HSE curve. Real distance is:

$x \cong 55 \times 5.150^{1/3} = 94.4$ m.

With TNO model

$V_0 = 10000/2(1 + 25) = 130{,}000\ m^3$ of mixture propane-air

$$L_0 = \left(\frac{130 \times 10^3 \times 3.5 \times 10^6}{1 \times 10^5} \right)^{1/3} = 165\ m$$

From (3.5) $r/L_0 = 0.6$ and $r = 98$ m.

≈≈≈≈≈≈≈≈≈≈≈≈≈≈≈

For the particular case of gas cloud detonation, some authors [35,36] proposed the following formulas for overpressure estimation:

$$\frac{\Delta p}{p_0} = 0.518 \times \left(\frac{r}{L_0} \right)^{-1.7} \qquad 0.29 < \frac{r}{L_0} < 1.088 \qquad (3.6)$$

$$\frac{\Delta p}{p_0} = 0.2177 \times \left(\frac{r}{L_0} \right)^{-1} + 0.1841 \times \left(\frac{r}{L_0} \right)^{-2} + 0.1194 \times \left(\frac{r}{L_0} \right)^{-3} \qquad \frac{r}{L_0} > 1.088$$

≈≈≈≈≈≈≈≈≈≈≈≈≈≈≈

4. DISPERSION MODELS

Dispersion models describe the airborne transport of toxic material vapours away from the accident site and consequently can predict the physical impact of accidental releases, such as those emerging from relief systems, pipe and tank ruptures.

Referring to the behaviour of the vapour cloud and to the duration of the release, six possible situations can be defined[2] :

---

[2]Releases can have quite different durations, so it is usual to consider two extreme release modes: instantaneous or continuous. Really the classification can not depend only on the duration of the release but also on the downwind position of the observer. In fact the plume from a release that is mantained for a finite time becomes detached from the source when the release terminates and the isolated plume thus formed is advected downwind and is subjected to longitudinal dispersion of its

behaviour of the vapour cloud	duration of release
Neutrally buoyant gas	instantaneous release (puff)
(Positively) buoyant gas	continuous release (plume)
Heavy (or negatively) buoyant gas	time varying continuous

Models for time varying continuous releases are complex and not frequently used in risk assessment and therefore will not be examined in the following paragraphs.

Furthermore the dispersion of very positively buoyant gases is of secondary importance, as such gases make for high layers of the atmosphere, and anyway could be described in a conservative way by using models for neutrally buoyant vapours (note that far from the source a gas is surely neutrally buoyant owing to the dilution).

Therefore in the following sections we will consider the models for four cases:

- continuous release (plume) of neutrally buoyant gas (evaporation from a pool,..)
- instantaneous release (puff) of neutrally buoyant gas (from relief valve,..)
- continuous release (plume) of heavy gas (evaporation from cryogenic pool, ..)
- instantaneous release (puff) of heavy gas (from the rupture of pressure vessel containing liquified gas,..).

A wide variety of parameters affect the atmospheric dispersion of toxic gases: wind velocity, atmospheric stability, ground conditions, buildings, water, trees, height of the release above ground level, momentum and buoyancy of the initial material released.

The first two parameters are assumed to represent the atmospheric turbulence in the classification proposed by Pasquill [38], which is synthetically explained in the following section.

4.1 Atmosphere and Pasquill stability classes

The dispersion of accidental or continuous releases concerns the atmospheric boundary layer, where a vertical temperature gradient (VTG) is present.

---

leading and trailing fronts. Therefore an observer will interpret the passage of the relased gas as a "puff". On the contrary a continuous sorce is necessarily related to the duration over which a steady concentration is observed at a particular position. It follows that a release which one observer would deem as 'continuous' may be deemed as 'istantaneous' by another observer further downwind. In [37,10] some criteria are proposed for distinguishing continuous and instantaneous releases. However in the common practice reference is only made to the duration of the release (defined instantaneous when the duration is less than 100 s).

Depending on the hour of the day, the season of the year, the solar radiation, this gradient can be negative (temperature decrease versus height) or positive (temperature increase versus height). The comparison of the ambient gradient with the adiabatic lapse rate (ALR = -0.98 °C/100 m) gives information about the turbulence degree of the atmosphere. (ALR is the rate temperature change with height for a parcel of dry air rising adiabatically.)

In **neutral** stability the gradient is equivalent to ALR, while, on the contrary, when

VTG is negative and its absolute value is greater than ALR, turbulence is enhanced and the air is **unstable (super-adiabatic condition)**

VTG is negative and its absolute value is lower than ALR, turbulence is suppressed and the air tends toward being **stable (sub-adiabatic condition)**

VTG is positive, turbulence is almost completely suppressed and the air is very **stable (inversion condition).**

Pasquill classes are reported in Tab. 4-1.

Class		Temperature gradient (°C/100 m)
A	extremely unstable	< - 1.9
B	moderately unstable	-1.9 < TG < -1.7
C	slightly unstable	-1.7 < TG < -1.5
D	neutral	-1.5 < TG < -0.5
E	slightly stable	-0.5 < TG < +1.5
F	moderately stable	> 1.5

Tab. 4-1 Pasquill classification

Wind speed and stability class should be obtained from local meteorological data whenever possible; if stability data are not available, the simple Tab. 4-2 permits atmospheric stability to be estimated from local sunlight and wind speed conditions.

Surface wind speed (m/s) at 10 m height	*Daytime insolation*			*Nighttime conditions*	
	Strong	*Moderate*	*Slight*	*Thin overcast or ≥ low 4/8 cloudiness*	*≤ 3/8 cloudiness*
< 2	A	A–B	B		
2–3	A–B	B	C	E	F
3–4	B	B–C	C	D	E
4–6	C	C–D	D	D	D
> 6	C	D	D	D	D

Tab. 4-2 Pasquill stability - meteorological conditions [39]

The influence of the temperature gradient is clearly proved in Fig. 4-1 which contains typical plumes: two drawings (referring to fumigation and lofting) are characterised by an inversion layer respectively above and below the plume.

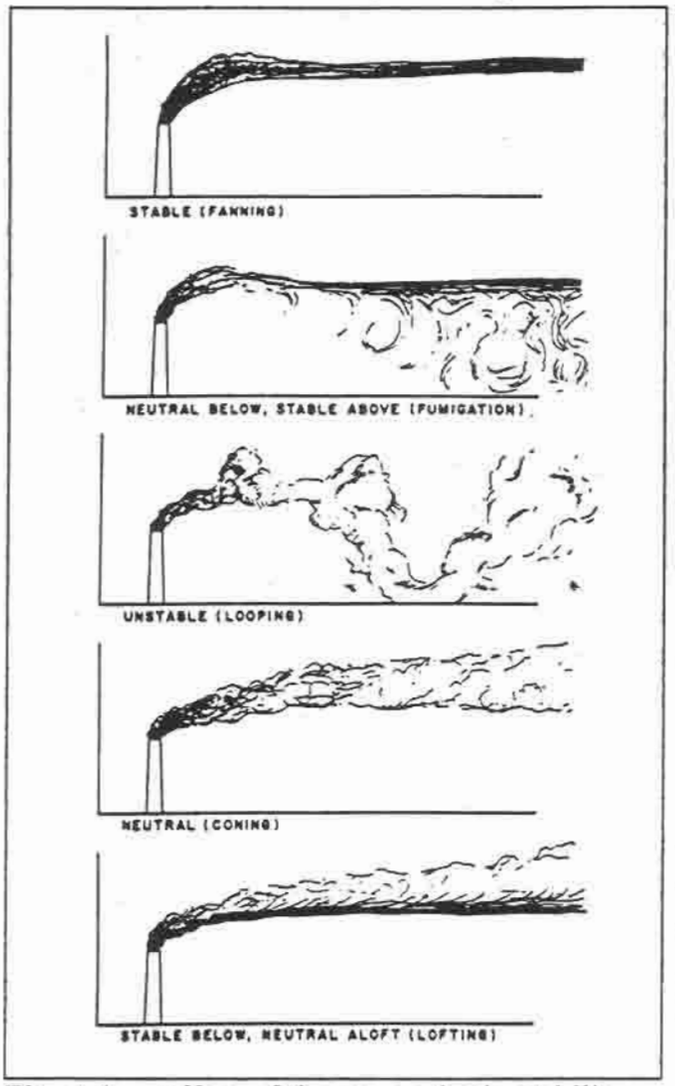

Fig. 4-1 Effect of the atmospheric stability on plume dispersion (from [40])

Wind data are normally quoted on the basis of 10 m height, but ground conditions affect the mechanical mixing at the surface and consequently the wind profile with height; a simple power relation is appropriate for u_z

$$u_z = u_{10}\left(\frac{z}{10}\right)^n \qquad (4.1)$$

where u_z , u_{10} are wind velocities at heights z and 10 m and n is the power correction coefficient, whose values are reported in Tab. 4-3,

stability class	Urban	Rural
A	.15	.07
B	.15	.07
C	.20	.10
D	.25	.15
E	.40	.35
F	.60	.55

Tab. 4-3 Wind speed correction coefficients

4.2 Effects of buoyancy and momentum of the release

The release is frequently in form of jet rather than a plume and near the release point its velocity differs greatly from the wind velocity. The jet entrains ambient

air due to shear, grows in size and becomes diluted. For a neutral buoyancy jet the upward momentum remains constant while its mass increases; therefore, if vertically released, it becomes bent over at a certain distance and dominated by the wind momentum. In case of positive buoyancy the upward momentum increases and the jet will behave like a plume.

In these cases the buoyancy and momentum of the material released increase the height of the release (source "effective" height is greater than source geometric height). The rises of jets (*plume rises*) have been studied by many researchers and their formulas can be found in several books [38,41,42].

For a heavy jet, upward momentum will decrease as it travels; at a maximum height the upward momentum disappears and then the jet will start to descend. The buoyancy release of heavy jets can be analysed with the model of Ooms [43] and is included in available codes, i.e. DEGADIS code [44].

4.3 Neutral Gas Dispersion

4.3.1 Neutral plume models

With the term plume we refer to continuous emissions, that are long in duration compared with the travel time (time for cloud to reach location of interest).

The Pasquill-Gifford model, here introduced, is widely used to predict concentration distribution in risk analyses.

This model assumes Gaussian dispersion in both the horizontal and vertical axes (Fig. 4-2).

For an elevated point source at an "effective" height H the concentration is

$$c(x,y,z) = \frac{\dot{m}}{2\pi\sigma_y\sigma_z u}\left[\exp\left(\frac{-y^2}{2\sigma_y^2}\right)\right]\left[\exp\left(\frac{-(z-H)^2}{2\sigma_z^2}\right)+\exp\left(\frac{-(z+H)^2}{2\sigma_z^2}\right)\right] \quad (4.2)$$

where

c = concentration (kg/m^3); $\dot{m}$ = emission rate (kg/s); σ_y, σ_z = dispersion coefficients (m), function of downwind distance x; u = wind velocity (m/s).

The ground is considered as a reflection surface, as no ground absorption or reaction is assumed. The effects of reflection are clearly depicted in Fig 4-3: curves at different H and at a fixed downstream distance are reported. It is worth noticing that the concentration has not a maximum at centreline height, as should be in a Gaussian distribution.

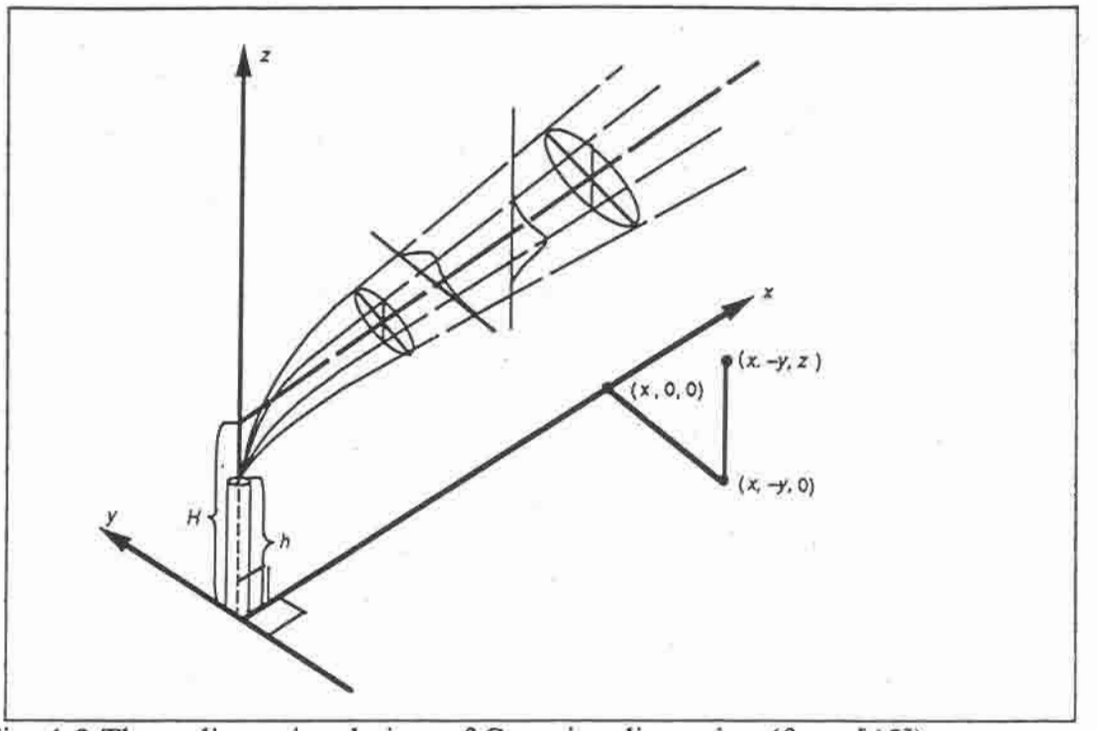

Fig. 4-2 Three-dimensional view of Gaussian dispersion (from [45])

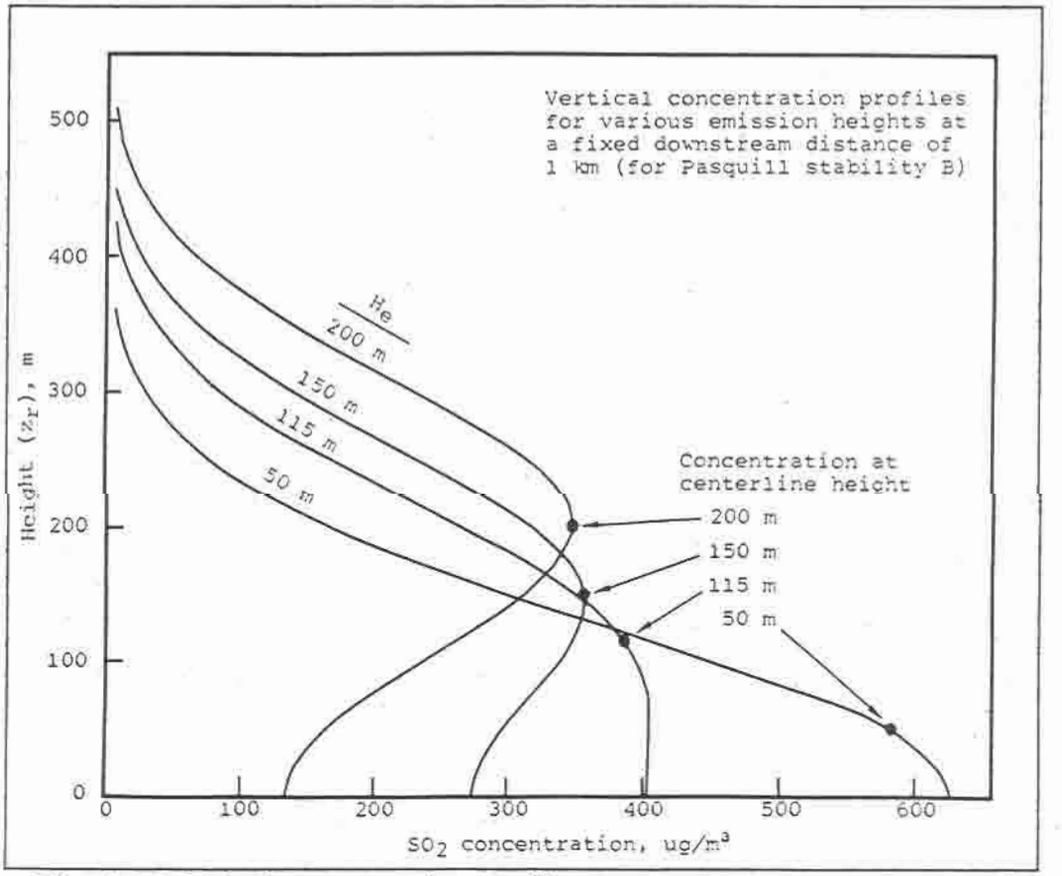

Fig. 4-3. Vertical concentration profiles

The dispersion coefficients are function of the downwind distance and were determined through a large variety of dispersion experiments. They can be

available as graphs (Fig. 4-4) or via predictive formulas [42,32,10].

The coefficients of predictive formulas reported in Tab. 4-4 are extracted from [10].

They refer to the expressions $\sigma_z = c' x^{d'}$ and $\sigma_y = a x^b$.

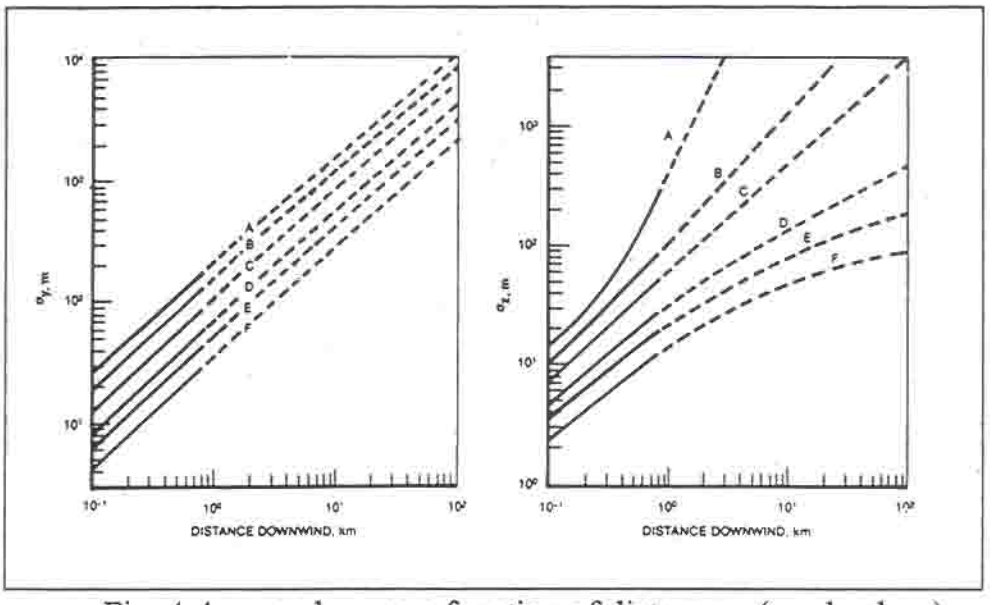

Fig. 4-4 σ_y and σ_z as a function of distance x (rural values)

Different coefficients are given for σ_z , because dispersion in vertical direction depends on ground roughness z_0 in m (the five values address respectively *flat land, cultivated land, land with sparse houses, residential area, industrial area or urban area*). The coefficients for σ_y imply a sampling time of 10 min: the meandering of wind is responsible of a local dilution if sampling times greater than 10 min are considered. In these cases a correction factor of $(t/10)^{0.2}$ must be applied.

class	a	b	c'	d'	c'	d'	c'	d'	c'	d'	c'	d'
			z_0 = .03		z_0 = .1		z_0 = .3		z_0 = 1		z_0 = 3	
A	.527	.865	.193	.932	.280	.900	.383	.873	.550	.842	.760	.814
B	.371	.866	.16	.881	.230	.850	.317	.822	.455	.792	.631	.763
C	.209	.897	.155	.83	.22	.800	.308	.771	.441	.740	.612	.712
D	.128	.905	.139	.791	.200	.760	.276	.732	.395	.701	.548	.673
E	.098	.902	.104	.761	.150	.730	.207	.702	.296	.671	.411	.643
F	.065	.902	.083	.701	.120	.670	.164	.642	.236	.611	.327	.583

Tab. 4-4 Coefficients for predictive formulas

The coefficients of Tab. 4-4 can be used only for "effective" heights less than 20 m. The restriction does not permit high source emissions to be evaluated, nevertheless the use is frequent in accidental releases as they are often emitted at low height (pools, pipes ands so on).

4.3.2 Neutral puff models

The Gaussian formula for puff emissions (short in duration compared with travel time or sampling time) is

$$c(x,y,z,t) = \frac{m}{(2\pi)^{3/2}\,\sigma_{xI}\,\sigma_{yI}\,\sigma_{zI}}\left[\exp\left(\frac{-(x-ut)^2}{2\sigma_{xI}^2}\right)\right]\left[\exp\left(\frac{-y^2}{2\sigma_{yI}^2}\right)\right]\times \left[\exp\left(\frac{-(z-H)^2}{2\sigma_{zI}^2}\right)+\exp\left(\frac{-(z+H)^2}{2\sigma_{zI}^2}\right)\right] \tag{4.3}$$

where

m = amount released (kg);
t = time elapsed after release (s);
σ_{xI}, σ_{yI}, σ_{zI} = dispersion coefficients (m).

It is usual to assume $\sigma_{xI} = 0.13$ x, $\sigma_{yI} = \sigma_y/2$, $\sigma_{zI} = \sigma_z$.

The eqn. 4-3 shows that, at a fixed point, the concentration varies with time and has a maximum when t = x/u.

4.3.3 Concluding remarks

The dispersion models here briefly explained use the assumption of *point source emission*, so that at the source they predict a concentration value of infinity and therefore will greatly over predict concentration in the near field . More complex formulas for other type of sources (linear and three-dimensional) can be found in [10,40]. To still apply them to a real source (e.g. a pool) with given dimensions, the concept of a virtual point source can be introduced: *the virtual point source is located upwind from the real source such that if a plume was originated at the virtual source it would disperse and match the dimensions or concentration at the real source* [10,46].

The output of plume and puff models are respectively the time averaged concentration and the concentration varying with time at specific locations (in the three spatial coordinates: x, y, z). This information are useful both for toxic and flammable releases.

In fact they allow ground isopleths to be plotted (*isopleth = line corresponding to a concentration of interest*) and included surfaces to be calculated, in this way giving basic information to the emergency planning of toxic cloud

dispersion. Moreover dispersion models permit to evaluate the mass of flammable material included in the isopleths at LEL (*Lower Explosion Limit*) and UEL (*Upper Explosion Limit*) which is the basic input to explosion models.

4.3.4 Sample problems

N.1

A toxic substance flow rate of 10 kg/s is emitted from a circular pool (diameter = 30 m). Assuming stability class D, u = 5 m/s, roughness = 0.1 m, determine

- the time averaged (10 min) concentration at a downwind distance of 1 km (at ground)
- the concentration at a distance of 120 m in lateral direction

≈≈≈≈≈≈≈≈≈≈≈≈≈≈≈

For H = 0, the concentration is

$$c(x,y,z) = \frac{\dot{m}}{2\pi\sigma_y \sigma_z u}$$ and in this case we have

$$c(1000,0,0) = \frac{10}{2\pi \times 0.128 \times 1000^{0.905} \times 0.2 \times 1000^{0.760} \times 5} = 0.252 \times 10^{-3}\, kg/m^3$$

Using the concept of virtual point source we would obtain c = 0.235 x 10^{-3} kg/m^3.
The concentration at downwind distance above calculated must be multiplied by

$$\left[\exp\left(\frac{-y^2}{2\sigma_y^2}\right)\right] = \left[\exp\left(\frac{-120^2}{2(0.128 \times 1000^{0.905})^2}\right)\right] = 0.242$$

and therefore c(1000,120,0) = 6.1 x 10^{-5} kg/m^3 .

≈≈≈≈≈≈≈≈≈≈≈≈≈≈≈

N.2

Chlorine is used in a particular chemical process. A source model study indicates that for a particular accident scenario 1.0 kg of chlorine will be released instantaneously. The release will occur at ground level. A residential area is 500 m away from the chlorine source. Determine

- the time required for the centre of the cloud to reach the residential area. (wind speed of 2 m/s)
- the maximum concentration of chlorine in the residential area and compare it

with the IDLH (Immediate Danger to Life and Health) for chlorine of 25 ppm. What stability condition and wind speed produces the maximum concentration?

≈≈≈≈≈≈≈≈≈≈≈≈≈≈≈

For a distance of 500 m and a wind speed of 2 m/s, the time required for the centre of the cloud to reach the residential area is

$t = x/u = 500 / 2 = 250$ s (4.2 min)

Very little time is available for emergency warning.

The maximum concentration will occur in the downwind direction (y, z = 0) at the previous calculated time. In this case, for H = 0, the concentration is

$$c(ut,0,0,t) = \frac{m}{(2\pi)^{3/2}\,\sigma_{xl}\,\sigma_{yl}\,\sigma_{zl}}$$

The stability conditions which maximise c require dispersion coefficients of minimum value. From Fig. 4-4 this occurs under stable conditions and from Tab. 4-2 this occurs at night with 2-3 m/s wind. From Tab.4.4 we have σ_{yI} = 17.7 /2 m, σ_{zI} = 7.7 m and σ_{xI} = 65 m.

$$c = \frac{1}{(2\pi)^{3/2}\,65 \times 8.8 \times 7.7} = 1.44 \times 10^{-3} \text{ kg / m}^3 =$$

$$= 14.4 \text{ mg / m}^3 \text{ (1 atm, 298 K)} \cong 5 \text{ ppm}$$

The concentration is of the same order of magnitude of IDLH.

4.4 HEAVY GAS DISPERSION

Many accidents in chemical plants, storage and transportation can lead to the dispersion of an heavy gas/vapour. Some examples are:

- the catastrophic breakage of a cryogenic tank causes the formation of a very cold pool and the emerging pure vapour has typically a greater-than-air density;
- the catastrophic breakage of a vessel containing liquefied gas brings to a violent flash vaporisation and mixing with air, consequently a cold and denser-than-air cloud will form;
- heavy gas jets result from breakages or leakages of pipes with liquefied gases.

These examples make clear that quite different source terms characterise the forming of dense gas and for this reason source modelling is, in some cases, included in heavy gas numerical codes (see also notes in par. 4.3).

The mechanisms of dense gas dispersion differ markedly from neutrally-buoyant

clouds, as several field experiments have confirmed as well [47,48]. These mechanisms are depicted in Fig. 4-5 and include three phases:

1. initial acceleration and dilution
2. dominance of internal (negative) buoyancy-gravity slumping
3. dominance of ambient turbulence (neutral buoyancy).

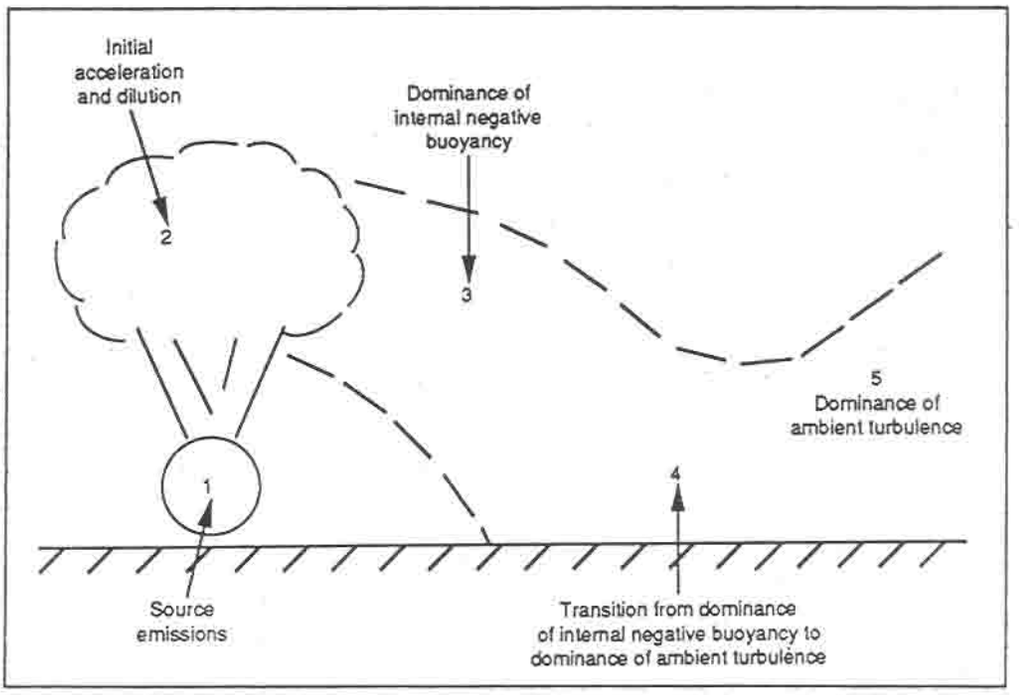

Fig. 4-5 Major regions in dense gas dispersion [1].

These regimes, synthetically described in the following section, are not always distinguishable and may overlap under different release situations.

4.4.1 Phases of the dense gas cloud evolution

Initial acceleration and dilution
During this phase the cloud formation takes place: the dense gas assumes its initial characteristics, that is shape, initial concentration, aerosol mass fraction, temperature, etc. The dominant factors that influence the clouds motion are the release conditions (source term) and the mean atmospheric flow.

This phase is crucial since it determines whether the cloud behaves subsequently as a dense or passive gas. Quantitative criteria are suggested in [37] for distinguishing passive behaviour. The cloud is passive when it results

for instantaneous source of volume V_0 $\quad (V_0^{1/3}\, g_0')^{1/2} \leq 0.2\, U_{ref}$

for continuous source of volume flow rate $\dot{V}_0$ $\quad (\dot{V}_0\, g_0' / D_s)^{1/3} \leq 0.15\, U_{ref}$

where U_{ref} is the velocity at 10 m height, D_s is the plume width and g'_0 is the reduced gravity acceleration

$$g_0' = g\,(\rho - \rho_a)/\rho_a$$

Dominance of internal (negative) buoyancy-gravity slumping
The cloud collapses (slumps) towards the ground and spreads horizontally while is being advected and diluted by the ambient flow. The slumping causes an increase of its diameter (or width) and a reduction of its height. Hence the dominant forces are the cloud (negative) buoyancy and the atmospheric flow field.
The gravity current-like motion during this phase of the dispersion is due to the density gradient in the horizontal direction and concentration profiles in cross direction are frequently uniform.

Dominance of ambient turbulence (neutral buoyancy).
First the turbulence in the ambient flow field affects the upper stratified layer of the cloud; progressively, as the cloud or plume travels downwind, the external turbulence interacts with an even larger part of it. The dilution proceeds until the dense gas concentration becomes so low that buoyancy effects are negligible and a neutral atmospheric dispersion results.

4.4.2 Heat exchanges between cloud and ambient

When the cloud is cold (i.e. evaporation from a pool of cryogenic liquid) and/or contains aerosols (i.e. ammonia cloud from a pressure storage breakage) heat exchanges between ambient and cloud become important and must taken into account in modelling dense gas dispersion. The different contributions are shown in Fig. 4-6.

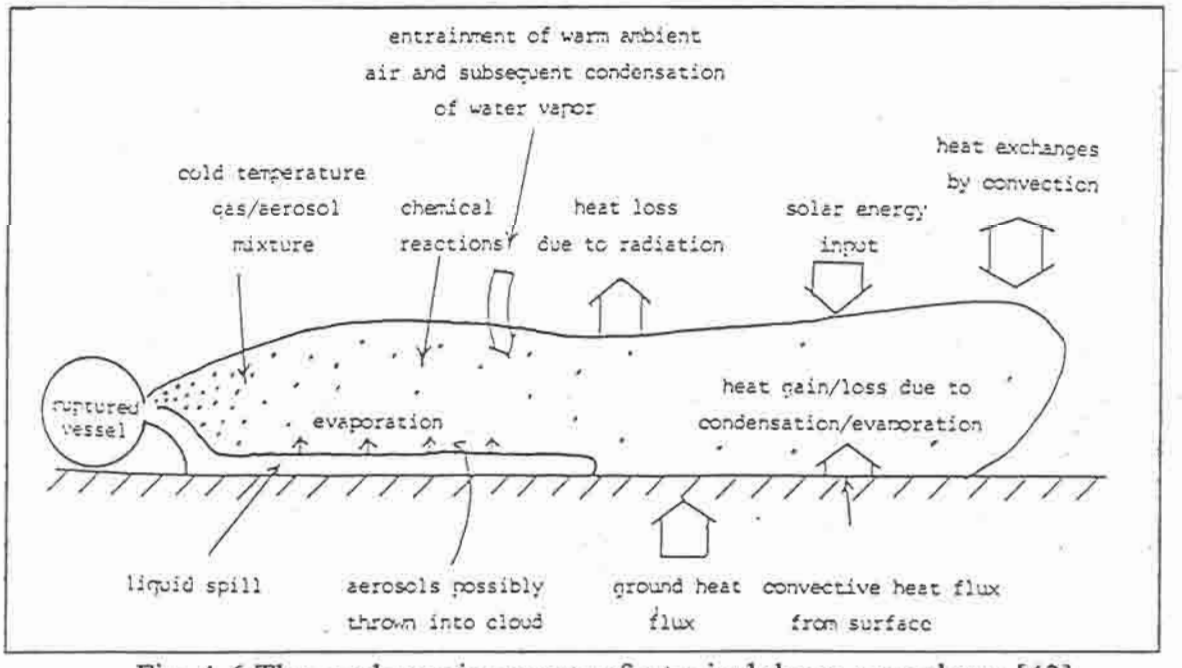

Fig. 4-6 Thermodynamic aspects of a typical dense gas release [42]

In such situations the heat balance equation must be coupled to mass balance equations in order to give a good mathematical description of the dispersion.

4.4.3 Mathematical MODELS for dense gas dispersion

Models are grouped usually in three categories:

- **similarity models**, which include **box models** and **advanced similarity models;**
- **intermediate** or depth-averaged **models;**
- **3-D,** time dependent, hydrodynamic **models (K-theory models).**

The *similarity models* are largely used in risk analysis calculations, as their mathematical complexity is low enough and small computational costs are required. These models use the following assumptions

- dispersion on flat terrain
- ground with a constant roughness
- no obstructions
- local concentration fluctuations are ignored
- the treatment of chemical reaction and deposition is limited.

Calculations of dispersion over variable terrain or obstacles require more detailed models which have a complex mathematical structure and an high cost of development and validation. Reviews of available models and codes for dense gas dispersion are given in [42,49], with a summary of 33 dense gas and neutral buoyancy models.

The similarity models, which are briefly described in the following sections, assume a specific concentration profile inside the cloud which remains unaltered during the dispersion.

4.4.3.1 Box models

The gas dispersion is simulated by modelling gravity slumping phase and passive phase.

Instantaneous release

The vapour cloud is treated as a single cylinder of radius R and height H containing vapour at uniform concentration and temperature. Both dimensions are functions of time (see Fig. 4-7.). Air mixes with the box as it dispersed downwind, therefore the volume increases.

The time behaviours of volume (V) , radius R and temperature T completely define the dispersion of the cloud. In fact these variables allow to obtain

cloud height $H = V/(\pi R^2)$

cloud mass $n = P_a V/(R_u T)$ $\quad n_a = n - m_s/M_s$ $\quad m = n_a M_a + m_s$

cloud density $\rho = m/V$ and contaminant concentration $c = m_s / V$

where

n	= total number of moles;
n_a	= number of air moles;
m_s	= contaminant mass;
M_a e M_s	= molecular weights of air and contaminant;
R_u	= gas constant
P_a	= atmospheric pressure.

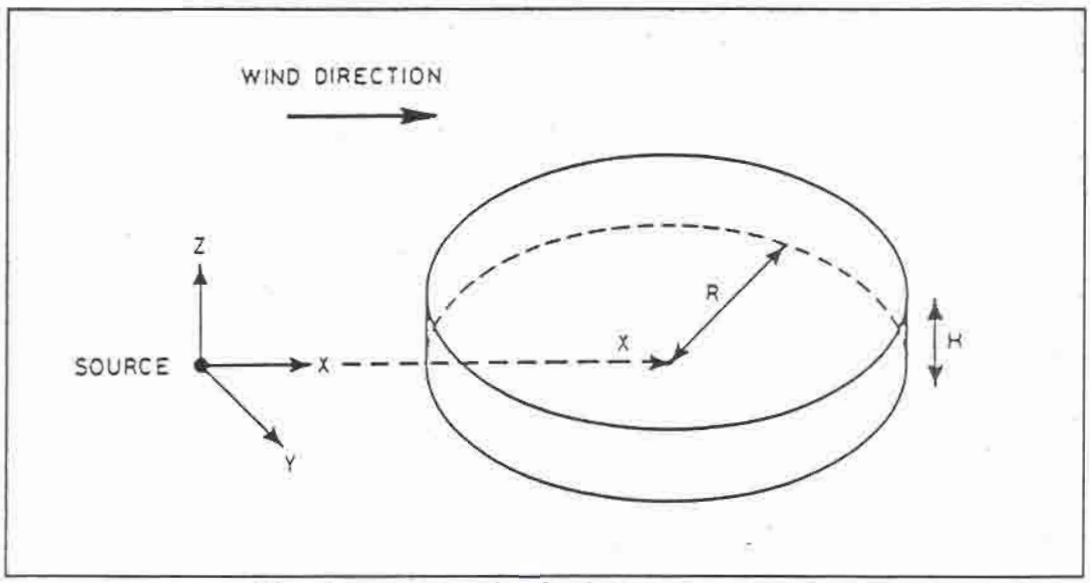

Fig. 4-7 Box model for instantaneous release

The required equations (mass balance, "slumping" and thermal balance), in adiabatic conditions (no aerosol is considered), are

$$\frac{dV}{dt} = (2\pi RH)u_E + \pi R^2 u_T \qquad (4.4)$$

$$u_f = \frac{dR}{dt} = \alpha(g' H)^{1/2} \qquad (4.5)$$

$$(T_a/T - 1)\, V + m_s/\rho_a\, (1 - \lambda - c_{ps}/c_{pa})\, T/T_a = \text{cost.},\ \lambda = 1 - M_a/M_s \qquad (4.6)$$

where T_a is the air temperature; c_{ps} and c_{pa} the specific heats of contaminant and air; u_f the front velocity; u_E the edge entrainment velocity and u_T the top entrainment velocity.

The displacement of the dense cloud by the wind is usually obtained from

$$x(t) = \int_0^t U_c \, dt \tag{4.7}$$

where x is the distance travelled by the cloud after time t from the release. Assuming a logarithmic variation of the wind velocity with height, we have

$$u_c = u_{*,10} \frac{\ln(z / z_0)}{\ln(10 / z_0)} \tag{4.8}$$

where $u_{w,10}$ is the wind velocity at 10 m height , z_0 is the roughness and z is a fixed height (usually = H/2).

The system can be solved once α and entrainment velocities are known. Extensive analyses of experimental data indicate that [50] $\alpha \cong 1.0$.

For the *edge entrainment velocity* the following relation has been proposed

$$u_E = \alpha_E u_f \tag{4.9}$$

which includes a dimensionless proportionality constant, whose value is often assumed equal to 0.7 [51,52,53]. However it is worth noting that other values are reported in literature, depending on the different experimental data used to calibrate the models.

The general mathematical formulation used for the *top entrainment velocity* is

$$u_T = \alpha_T v f(Ri_b) \qquad (4.10) \qquad Ri_b = \frac{g' l}{v^2} \qquad (4.11)$$

where α_T is a dimensionless coefficient, v is a turbulent velocity scale, l a length scale and $f(Ri_b)$ is function of a bulk Richardson number, which compares buoyancy forces with inertial forces.

Equations (4.10) and (4.11) are based on laboratory experiments on vertical entrainment in stratified flows. In most models is

$$f(Ri_b) = Ri_b^{-1} \tag{4.12}$$

while v and l values may differ, as shown in the following table

v	l_S	
u^*	H	u^* = friction velocity [54,55]
u_l	$H_r(H/H_r)^{0.48}$	u_l = turbulence vel.; H_r = 30 .2 m [56]
$a_3 U_{w,10}$	$5.88H^{0.88}$	a_3 = 0.3 unstable atm.; 0.24 neutral atm., 0.16 stable atm. [53]

The proportionality constant α_T assumes different values depending on the model calibration, but, usually, is in the range 0-1.

As previously said, instantaneous releases of heavy gases often have low temperature at emission and the dispersion cannot be assumed isothermal or adiabatic. The energy balance must include heat exchanges by convection with ground, by radiation with sun and so on. In DENZ code [16] natural convection only is considered.

Continuous release

A release of long duration at low velocity (vapour emerging from a pool, ..) is modelled as a plume, of contaminant flow rate $\dot{m}_s$, with a rectangular cross section of width $2L(x)$ and height $h(x)$, where x is the downwind distance from the source (Fig. 4-8). Plume density, temperature and composition are assumed constant at each cross section.

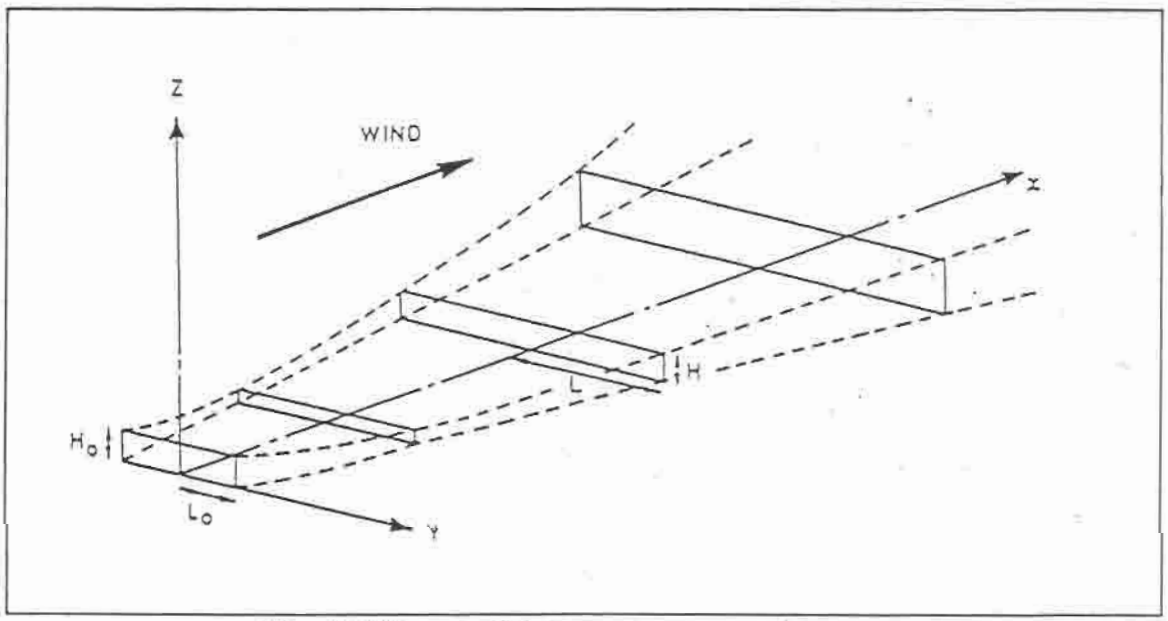

Fig. 4-8 Box model for continuous release

A system of three equations determines the behaviour of half-width, entrained air flow rate and temperature of the plume with the distance from the source.

The equation system included in CRUNCH [57] model is

$$\frac{dL}{dx} = k\left[\frac{\rho-\rho_a}{\rho_a}\frac{g\dot{V}}{2Lu_c^3}\right]^{1/2} \tag{4.13}$$

$$\frac{d\dot{m}_a}{dx} = 2L\rho_a u_T + \frac{\rho_a \dot{V}}{L}\alpha_E \frac{dL}{dx} \tag{4.14}$$

$$\left(\dot{m}_a c_{p,a} + \dot{m}_s c_{p,s}\right)\frac{dT_c}{dx} = \left(T_a - T_c\right)c_{p,a}\frac{d\dot{m}_a}{dx} + 2L\dot{q}''_{gr} \tag{4.15}$$

where $\dot{q}''_{gr}$ is the thermal flux exchanged with the ground surface.

The velocities of air entrainment from top and edges have the same expressions adopted for instantaneous release (eqn 4.10 and 4.11), but proportionality constants differ (in CRUNCH model $u_E = 0.6$ and $u_T = 0.2$).

Criteria for transition to passive(neutral) dispersion

The used criteria can be grouped into three kinds [42]:

- density perturbation $(\rho - \rho_a) / \rho \leq 0.01$
- bulk Richardson number ≤ 1 (critical value)
- frontal velocity U_f becomes of the order of magnitude of the friction velocity.

At the transition point box models change over to a Gaussian puff or plume models (sec. 4.3.1 and 4.3.2). Virtual point source concepts are used to make transition.

Remarks on box models

The synthetically described models assume that release sources have known cylindrical or rectangular shape. The initial dimensions must be defined through proper "source term" models depending on accident type. For "cold" or "warm" catastrophic ruptures reference can be made to the treatment given in [58] and [10] respectively, while continuous releases require pool models (for cryogenic liquids) or vapour jets models (see sec.1.1).

It is worth noting that box models assume that the contaminant is completely contained in a dense puff (a cylinder) or plume of finite dimensions, thus the contaminant concentration has a discontinuity at boundaries. This simplification is removed in the *advanced similarity models*.

4.4.3.2 Advanced similarity models

These models, which can also treat time-varying releases, use more realistic assumptions to describe the distribution of the contaminant downwind the source: vertical and lateral variations of concentration are taken into account assuming that the cloud consists of a central homogeneous core in which dispersion occurs only vertically and of an external region where Gaussian concentration profiles take place.

The most characteristic model of this kind is the Colenbrander model [59]. It is named HEGADAS and has been modified in [60] and later by Spicer and Havens [61]. The main contents of this last adaptation, which is called DEGADIS, will be briefly explained in the following. A complete knowledge of the mathematical treatment is obtainable referring to the bibliography.

DEGADIS can be separated into three parts:

- the dense gas cloud formation and growth, either from an evaporating liquid pool (continuous release) or from a specified gas volume (instantaneous release);
- the downwind dispersion of a steady-state release;
- the transient release simulation.

For sake of shortness, attention will be only devoted to the second phase, the most crucial one.

The downwind dispersion of a steady-state release (continuous source)

The model deals with the dispersion of gas entrained into the wind field from an idealised rectangular shape source of width 2B and length L. The following similarity profiles for the time-mean wind velocity u_x in the atmospheric surface layer and for the vapour concentration C in the heavy gas plume have been adopted

$$u_z = u_0 \left(\frac{z}{z_0} \right)^{\alpha} \tag{4.16}$$

$$C(x,y,z) = C_A(x) \exp\left[-\left(\frac{|y| - b(x)}{S_y(x)} \right)^2 - \left(\frac{z}{S_z(x)} \right)^{1+\alpha} \right] \quad for\ |y| > b \tag{4.17}$$

$$C(x,y,z) = C_A(x) \exp\left[-\left(\frac{z}{S_z(x)} \right)^{1+\alpha} \right] \quad for\ |y| \le b \tag{4.18}$$

Fig. 4-9 gives a graphical description of an iso-concentration contour.

The x-dependent variable C_A (ground level, centreline gas concentration), b (half-width of the horizontally homogeneous centre section) S_y and S_z (lateral and vertical dispersion parameters) are to be determined in order to evaluate the concentration profile.

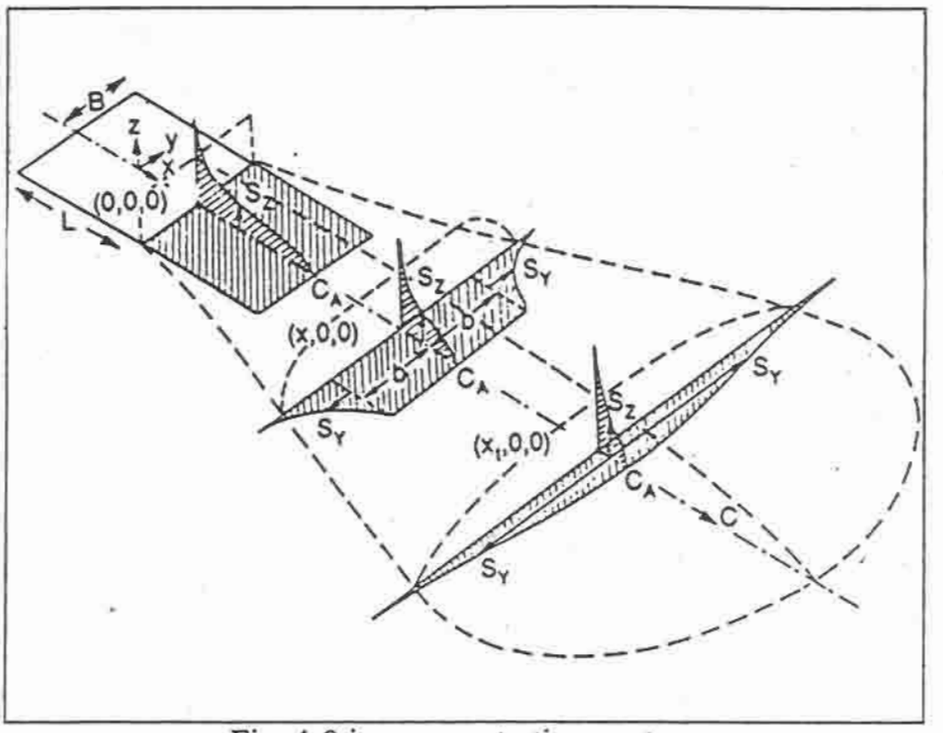

Fig. 4-9 iso-concentration contours

Their values can be obtained form the solution of the following system of equations

$$\frac{d}{dt}\left[B_{eff}\left(\frac{S_z}{z_0}\right)^{1+\alpha}\right]=\frac{k}{z_0}\frac{u_*}{u_0}\frac{(1+\alpha)^2\,B_{eff}}{\Phi(Ri_b)} \quad \text{with} \quad Ri_b=g\frac{\rho-\rho_a}{\rho_a}\frac{H_{eff}}{u_*^2} \tag{4.19}$$

$$S_y\frac{dS_y}{dx}=\frac{4\beta}{\pi}B_{eff}^2\left[\frac{\delta\sqrt{\pi/2}}{B_{eff}}\right]^{\frac{1}{\beta}} \tag{4.20}$$

$$\frac{dB_{eff}}{dx}=C_E\left[\frac{gz_0\Gamma^3\left(\frac{1}{1+\alpha}\right)}{u_0^2(1+\alpha)}\right]^{\frac{1}{2}}\left(\frac{\rho-\rho_a}{\rho_a}\right)^{\frac{1}{2}}\left(\frac{S_z}{z_0}\right)^{\left(\frac{1}{2}-\alpha\right)} \tag{4.21}$$

$$E=\int_0^{\infty}\int_{-\infty}^{\infty}Cu_x\,dydz=2C_A\left(\frac{u_0z_0}{1+\alpha}\right)\left(\frac{S_z}{z_0}\right)^{\frac{1}{2}}B_{eff} \tag{4.22}$$

where K is the von Karman constant, β and δ are constants in the experimentally determined expression for σ_y, Γ is the gamma function and B_{eff} and H_{eff} are respectively the effective half-width and height of the plume defined by:

$$B_{eff} = b + \frac{\sqrt{\pi}}{2} S_y \qquad H_{eff} = \frac{\Gamma\left(\frac{1}{1+\alpha}\right)}{1+\alpha} S_z \tag{4.23}$$

When x is large and b becomes zero the Pasquill correlation is used in order to calculate the lateral dispersion parameter.

With regard to the system of equations, it can be noted that:

- equation (4.19), which is derived from the diffusion equation, contains a bulk Richardson number Ri_b. The function $\phi(Ri_b)$ describes the influence of a density stratification on the diffusion in the vertical direction and is obtained from experimental data;
- equation (4.20) is a rewriting of the simple two-dimensional diffusion equation which is assumed to hold also if b is not zero;
- equation (4.21) describes the gravitational lateral spreading of the dense plume due to the difference in density between the plume and the surrounding air;
- equation (4.22) is the integral mass balance for the contaminant.

It is worth noting that the density of the vapour-air mixture must be known for the evaluation of the Richardson number Ri_b which, as said, appears in the expression describing the gravitational spreading of the plume. Then an energy balance must be written to correctly evaluate the cloud temperature and consequently the cloud density. In [61,62] heat fluxes from ground and from entrained air are considered.

4.4.3.3 Numerical codes for dense gas dispersion

Several numerical codes for dense gas dispersion modelling are described in the open literature and an interesting comparison between fourteen codes and eight experiments is reported in [63]. A list, surely not exhaustive, of these codes contains: CHARM [64], FOCUS [65], GASTAR 2.22 [66], PHAST 2.01 [67], SLAB [68], TRACE II, OME [69], DENS1 [70], BOX [71], WHAZAN [72], HGSYSTEM.

5. VULNERABILITY MODELS

5.1 Introduction

The models reported in the previous paragraphs allow to calculate the physical impacts of accidents, e.g. the spatial distribution of heat radiation for fires, of blast overpressure for explosions, of concentration for dispersions. The consequences of accidents depend on the object of the study; thus they may be expressed either as *deaths or injuries* for assessing effects on human beings or as *monetary losses*, if damages on structures and buildings must be evaluated.

Nevertheless, to compare risks of different types, a common unit of consequence measure must be used: the predominant comparison criterion for establishing damages on people is generally based on *fatalities*.

A method of assessing consequences is the *direct effect model*, which uses predetermined criteria: for example death is assumed to result if an individual is exposed, for a known duration, to a certain concentration of toxic gas or to a fixed radiant flux. Obviously with these criteria also safety distances can be evaluated. Some reference values for the effects of thermal radiation, overpressure and toxic exposure are reported in App. I.

In reality the consequences may not take the form of discrete functions but may instead conform to probability distribution functions. The more largely used statistical method is the probit (*prob*ability un*it*) method described by Finney [73] that introduces a generalised relationship useful for any variable whose probabilistic outcome can be defined by a normal (Gaussian) distribution. So this method can be used to assess any effect by establishing a statistical correlation between a "damage load (**dose**)" and the percentage of people affected to a specific degree (**response**). *The percentage of people affected* can be also considered as *the probability of an individual* to suffer a damage.

Response versus dose curves can be drawn for a wide variety of exposure, including exposure to heat radiation, overpressure, toxic concentration, impact and sound.

We can conclude these considerations observing that the use of the probit method is a good tool to obtain information about the magnitude of the damage, as it permits to establish the distribution of the percentage of people affected by a damage (usually death), i.e. the probability of damage, in a specified area around the accident source.

5.2 The probit method

The relationship between the probability P and the probit variable Y is:

$$P = \frac{1}{\sqrt{2\pi}} \int_{-\infty}^{Y-5} \exp(-u^2/2)\, du \qquad (5.1)$$

thus Y is a random variable defined by a normal distribution with a mean value of 5 and a standard deviation of 1 and P is its cumulative function. The relationship 5.1 is plotted in Fig. 5-1 and tabulated in Tab. 5-1 .

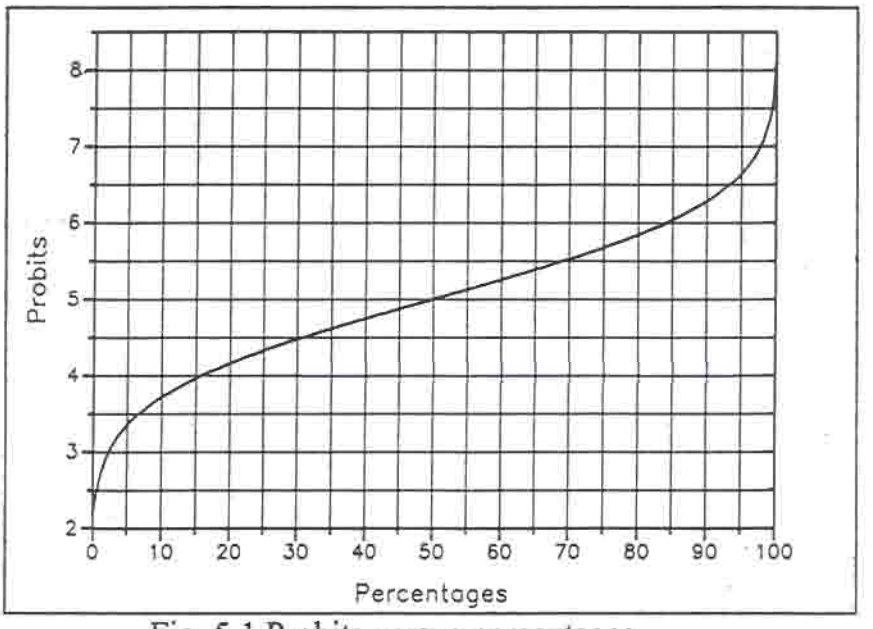

Fig. 5.1 Probits versus percentages

%	0	1	2	3	4	5	6	7	8	9
0	—	2.67	2.95	3.12	3.25	3.36	3.45	3.52	3.59	3.66
10	3.72	3.77	3.82	3.87	3.92	3.96	4.01	4.05	4.08	4.12
20	4.16	4.19	4.23	4.26	4.29	4.33	4.36	4.39	4.42	4.45
30	4.48	4.50	4.53	4.56	4.59	4.61	4.64	4.67	4.69	4.72
40	4.75	4.77	4.80	4.82	4.85	4.87	4.90	4.92	4.95	4.97
50	5.00	5.03	5.05	5.08	5.10	5.13	5.15	5.18	5.20	5.23
60	5.25	5.28	5.31	5.33	5.36	5.39	5.41	5.44	5.47	5.50
70	5.52	5.55	5.58	5.61	5.64	5.67	5.71	5.74	5.77	5.81
80	5.84	5.88	5.92	5.95	5.99	6.04	6.08	6.13	6.18	6.23
90	6.28	6.34	6.41	6.48	6.55	6.64	6.75	6.88	7.05	7.33
%	0.0	0.1	0.2	0.3	0.4	0.5	0.6	0.7	0.8	0.9
99	7.33	7.37	7.41	7.46	7.51	7.58	7.65	7.75	7.88	8.09

Tab. 5-1 The transformation from percentages to probits (from [1])

The relationship 5.1 transforms the sigmoid shape of the curve response (P) versus dose (V) into a straight line if the variable Y, instead of P, is plotted versus logV. The probit variable is then computed from

$$Y = k_1 + k_2 \ln V \quad (5.2)$$

Tab. 5-2 lists a variety of values of k_1 and k_2 for different type of exposures; the causative factor represents the dose V.

Type of injury or damage	Causative variable	Probit parameters k_1	k_2
Fire:			
Burn deaths from flash fire	$t_e I_e^{4/3}/10^4$	−14.9	2.56
Burn deaths from pool burning	$tI^{4/3}/10^4$	−14.9	2.56
Explosion:			
Deaths from lung hemorrhage	p^o	−77.1	6.91
Eardrum ruptures	p^o	−15.6	1.93
Deaths from impact	J	−46.1	4.82
Injuries from impact	J	−39.1	4.45
Injuries from flying fragments	J	−27.1	4.26
Structural damage	p^o	−23.8	2.92
Glass breakage	p^o	−18.1	2.79
Toxic release:			
Chlorine deaths	$\Sigma C^{2.75} T$	−17.1	1.69
Chlorine injuries	C	−2.40	2.90
Ammonia deaths	$\Sigma C^{2.75} T$	−30.57	1.385

t_e = effective time duration (s); I_e = effective radiation intensity (W/m^2); t = time duration of pool burning (s); p^o = peak overpressure (Pa); J = impulse (Pa s).

Probit models to estimate lethal thermal doses from pool and flash fire and lethal overpressure doses from UVCE and VCE are in general based on nuclear explosion data.

Toxic dose is usually defined in terms of concentration raised to a power multiplied by the duration of exposure (C^n t), with n ranging from 0.6 to 3 [32] . For continuous releases toxic dose may be calculated directly; for time-varying (puff) releases it should be estimated by the following integration

$$V = \int_{t_o}^{t_{end}} C^n \, dt \quad (5.3)$$

where

C = concentration (in ppm); $t = t_{end} - t_o$ exposure time (min).

Constants for lethal toxicity probit equations are provided in Tab. 5-3 for twenty

pure substances.

Substance	a (ppm)	b (ppm)	n (min)
Acrolein	−9.931	2.049	1
Acrylonitrile	−29.42	3.008	1.43
Ammonia	−35.9	1.85	2
Benzene	−109.78	5.3	2
Bromine	−9.04	0.92	2
Carbon monoxide	−37.98	3.7	1
Carbon tetrachloride	−6.29	0.408	2.50
Chlorine	−8.29	0.92	2
Formaldehyde	−12.24	1.3	2
Hydrogen chloride	−16.85	2.00	1.00
Hydrogen cyanide	−29.42	3.008	1.43
Hydrogen fluoride	−35.87	3.354	1.00
Hydrogen sulfide	−31.42	3.008	1.43
Methyl bromide	−56.81	5.27	1.00
Methyl isocyanate	−5.642	1.637	0.653
Nitrogen dioxide	−13.79	1.4	2
Phosgene	−19.27	3.686	1
Propylene oxide	−7.415	0.509	2.00
Sulfur dioxide	−15.67	2.10	1.00
Toluene	−6.794	0.408	2.50

Tab. 5-3 Constants for lethal toxicity (from [1])

Probit equations parameters are usually derived from animal experiments; in some cases, approximate estimations are available from historical toxic accidents which complement animal data. Experiments usually concern groups of rats or mice and there is no definitive correlation to relate human and animal responses as the relationship between species often depends on the substance. A used approach requires extrapolation procedures that account for differences in air intake and body weight [74].

In [75] methods for the measurement of possible damages on people and objects are explained with large details. In addition a chapter is devoted to treat an argument of great importance in the QRA (Quantified Risk Assessment) procedure: the ***protection*** *against toxic substances by remaining* ***indoors*** *and its evaluation.*

≈≈≈≈≈≈≈≈≈≈≈≈≈≈≈

5.3 Sample problems

N.1

Determine the thermal flux necessary to cause 50% fatalities for 10 and 100 seconds of exposure. Using probit method, eqn. 5.2 can be rearranged to solve for the radiation intensity I

$$I = \left[\frac{10^4 \exp[(Y+14.9)/2.56]}{t}\right]^{3/4}$$ where for 50% fatality Y = 5.0 (Tab.5-1).

The results are

t (s)	I (kW/m ^{2})
10	61
100	11

This example demonstrates the importance of duration of exposure, especially for short duration incidents such as BLEVE's and suggests that a fixed criterion is inappropriate for such incidents. For prolonged exposures a specific criterion could seem suitable, but in such cases the possibility of escape will play an important role.

N.2

Determine the probability of death from a 20-min exposure to 400 ppm of chlorine.

Using data of Tab. 5-3

$$Y = -8.29 + 0.92 \ln(400^2 \times 20) = 5.49$$

The probability of death, referring to Tab. 5-1, is 69%.

≈≈≈≈≈≈≈≈≈≈≈≈≈≈≈

APPENDIX I

Effects of thermal radiation on people and structures

Radiation intensity (kW/m^2)	*Observed effect*
37.5	Sufficient to cause damage to process equipment
25	Minimum energy required to ignite wood at indefinitely long exposures (nonpiloted)
12.5	Minimum energy required for piloted ignition of wood, melting of plastic tubing
9.5	Pain threshold reached after 8 s; second degree burns after 20 s
4	Sufficient to cause pain to personnel if unable to reach cover within 20 s; however blistering of the skin (second degree burns) is likely; 0% lethality
1.6	Will cause no discomfort for long exposure

Damages produced by explosion overpressure (1 bar = 14.5 psi)

Pressure (psig)	*Damage*
0.02	Annoying noise (137 dB if of low frequency 10–15 Hz)
0.03	Occasional breaking of large glass windows already under strain
0.04	Loud noise (143 dB), sonic boom glass failure
0.1	Breakage of small windows under strain
0.15	Typical pressure for glass breakage
0.3	"Safe distance" (probability 0.95 no serious damage beyond this value); projectile limit; some damage to house ceilings; 10% window glass broken
0.4	Limited minor structural damage
0.5–1.0	Large and small windows usually shattered; occasional damage to window frames
0.7	Minor damage to house structures
1.0	Partial demolition of houses, made uninhabitable
1–2	Corrugated asbestos shattered; corrugated steel or aluminum panels, fastenings fail, followed by buckling; wood panels (standard housing) fastenings fail, panels blown in
1.3	Steel frame of clad building slightly distorted
2	Partial collapse of walls and roofs of houses
2–3	Concrete or cinder block walls, not reinforced, shattered
2.3	Lower limit of serious structural damage
2.5	50% destruction of brickwork of houses
3	Heavy machines (3000 lb) in industrial building suffered little damage; steel frame building distorted and pulled away from foundations
3–4	Frameless, self-framing steel panel building demolished; rupture of oil storage tanks
4	Cladding of light industrial buildings ruptured
5	Wooden utility poles snapped; tall hydraulic press (40,000 lb) in building slightly damaged
5–7	Nearly complete destruction of houses
7	Loaded train wagons overturned
7–8	Brick panels, 8–12 in. thick, not reinforced, fail by shearing or flexure
9	Loaded train boxcars completely demolished
10	Probable total destruction of buildings; heavy machines tools (7000 lb) moved and badly damaged, very heavy machine tools (12,000 lb) survived
300	Limit of crater lip

Relatively high blast overpressure (> 15 psig) are necessary to produce fatality (due to lung haemorrhage). Instead the major threat is produced by missiles or by whole body translation [76].

Toxicity data (IDLH) for some substances

Many useful data on toxicity due to the inhalation exposure are available [75]: in the following some IDLH values are reported as they are often used in risk analysis.

IDLH the maximum airborne concentration of a substance to which a healthy male worker can be exposed for as long as 30 min and still be able to escape without loss of life or irreversible organ system damage.

Substance	**IDLH (mg/m^3)**
Acetic acid	2502
Acetic anhydride	4254
Acrylonitrile	8843
Aminobenzene	388
Aminomethane	129
Ammonia	355
n-Amyl alcohol	551
Aniline	388
Nitric acid	263
Benzene	6510
Bromine	67
n-Butyl carbinol	551
Calcium oxide	139
Carbon disulphide	1586
Carbolic acid	20
Chlorine	74
Chloroethane	53700
Chloroform	4974
Chloromethane	21000

References

1. *Guidelines for chemical process quantitative risk analysis,* Centre for Chemical Process Safety, AIChE, New York, 1989.
2. R.H. Perry, D. Green (eds.), *Perry's chemical engineering handbook,* 6th edition, McGraw-Hill, New York, 1984
3. C. Crane, *Flow of fluids through valves, fittings and pipe, metric edition-SI units,* Technical paper No. 410M, Crane, New York, 1981.
4. H.K. Fauske, M. Epstein, *Source term considerations in connection with chemical accidents and vapour cloud modelling,* J. Loss Prev. Process Ind., 75, 1988
5. D.S. Nielsen, *RISO Laboratory,* J. Loss Prev. Process Ind., July, 1991.
6. J.C. Leung, *A generalised correlation for one-component homogeneous equilibrium flashing choked flow,* AIChE J., 1986
7. S.F. Hall, *SRD Report R127,* 1978.
8. K.S. Mudan, *Gravity spreading and turbulent dispersion of pressurised releases containing aerosols*, IUTAM Symposium, Delft, Olanda, 1983.
9. V. Iannello et al., *Aerosol research program: improved source term. definition for modelling the ambient impact of accidental release of hazardous liquids*, 6th Int. Sym. Loss Prevention and Safety Promotion in the Process Industries, Oslo, 1989.
10. *Methods for the calculation of physical effects, CPR 14E,* TNO, Voorburg, The Netherlands, November 1988.
11. D. M. Webber, *GASP code*, J Loss Prev. Process Ind., January 1991.
12. P.Leonelli, C, Stramigioli, G. Spadoni, *The modelling of pool vaporisation,* Praga, CHISA Congress, 1993.
13. P.H. Thomas, *The size of flames from natural fires,* 9th Int. Sym. on Combustion, Academic Press, New York, 1963.
14. K.S. Mudan, *Thermal radiation hazards from hydrocarbon pool fires,* Proc. Energy Combust. Sci. 10(1), 1984.
15. H.C. Hottel, A.F. Sarofim, *Radiative transfer,* McGraw Hill, New York, 1967.
16. America Gas Association, *LNG safety research program,* Report IS 3-1, Columbus, OH, 1974.
17. C.M. Pieterson, S.C. Huaerta, *Analysis of the LPG incident in San Juan Ixhuatepec, Mexico City, 19 Nov. 1984,* TNO Report B4-0222, Apeldoorn, The Netherlands, 1985.
18. D.R. Bagster, *Pool and jet fires,* Major Industrial Hazards Project, Warren Centre for Advanced Engineering, University of Sidney, Australia, 1986.
19. API, *Guide for pressure-relieving and depressuring systems,* API recommended practice 521, end edition, America Petroleum Institute, Washington, D.C., 1982.
20. J. Hustad, O.K. Sonju, *Radiation and size scaling of large gas and gas-oil diffusion flames,* 10th Intern. Coll. on Dynamics of Explosions and Reactive Systems, Berkeley, 1986.

21. W.R. Hawthorne, et al., *Mixing and combustion in turbulent fuel jets,* Third Sym. Int. on Combustion, Baltimore, 1949.
22. T. Baron, *Reactions in turbulent free jets - the turbulent diffusion flame,* Chem. Eng. Progr. 60, 73, 1954
23. J. Moorhouse, M.J. Pritchard, *Thermal radiation hazards from large pool fires and fireballs - a literature review,* The Assessment of Major Hazards. IChemE Symposium Series No. 71, IChemE, Rugby, UK, 1982.
24. R.M. Pitblado, *Consequence models for BLEVE incidents,* Major Industrial Hazards Project, Warren Centre for Advanced Engineering, University of Sidney, Australia, 1986.
25. R.W. Prugh, *Quantitative evaluation of BLEVE hazards,* AIChE Loss Prevention Symp., paper No. 74e, AIChE Spring National Meeting, New Orleans, March 6-10, 1988.
26. Association of American Railroads, *Analysis of tank car tub rocketing in accidents,* AAR Report R130, Washington , D.C. 1973.
27. P.L. Holden, A.B. Reeves, *Fragment hazards from failures of pressurised liquified gas vessels,* Assessment and Control of Major Hazards, IChemE Symp. Series No. 93, IChemE, Rugby, UK, 1985.
28. I. Hymes, *The physiological and pathological effects of thermal radiation,* UKAEA Safety and Reliability Directorate, Report SRD R275, Culcheth, UK, 1983.
29. S.J. Brown, *Energy release protection for pressurised systems, part I review of studies into blast and fragmentation,* Applied Mechanics Reviews 38, 1985.
30. NFPA, *Guide for explosion venting,* NFPA 68, National Fire Protection Association, Quincy, MA, 1988.
31. D.A. Decker, *An analytical method for estimating overpressure from theoretical atmospheric explosions,* Annual Meeting of the National Fire Protection Association and Society of Fire Protection Engineers, May 23, 1974.
32. F.P. Lees, *Loss Prevention in the process industries,* 2 volumes, Butterworths, London, Boston, 1980.
33. B.J. Wiekema, *Vapour cloud explosions,* chapter 8 in Methods for the Calculation of the Physical Effects of the Escape of Dangerous Materials: Liquid and Gases, The Yellow Book, Apeldoorn, The Netherlands, 1979.
34. Health and Safety Executive, *Advisory Committee on Major Hazards: second report,* HMSO, London, UK, 1979.
35. S.M. Kogarko, V.V. Aduskin, A.G. Lyamin, *An investigation of spherical detonations of gas mixtures,* Int. Chem. Eng., 6, 1966.
36. S.R. Brinkley, *Determination of explosion yields,* AIChE Loss Prevention, 3, 1966.
37. R.E. Britter, J. McQuaid, *Workbook on the Dispersion on Dense Gases,* HSE Contract Research Report No.17/1988. HSE, Sheffield, UK, 1988.
38. M.R. Baychock, *Fundamentals of stack gas dispersion,* M.R. Baychock,

CA, 1979.
39. F.A. Gifford, *Atmospheric dispersion models for environmental pollution applications*, Proceedings on Lectures on Air Pollution and Environmental Impact Analyses, AMS Workshop on Meteorology and Environmental Assessment, AMS, Boston, 1975.
40. D.H. Slade (ed.), *Methodology and atomic energy*, Report No. TID-24190, U.S. Atomic Energy Commission, Division of Technical Information, Washington D.C., 1968, (available from NTIS).
41. G.A. Briggs, *Plume rise predictions*, Proc. of the Lectures on Air Pollution and Environmental Impact Analyses, America Meteorological Society, Boston, MA, 1975.
42. S.R. Hanna, P.J. Drivas, *Guidelines for use of vapour cloud dispersion models, Center for Chemical Process Safety*, AIChE, New York, 1987.
43. G. Ooms et al., *Loss Prevention and Safety Promotion in the Process Industries*, Elsevier Scientific Publishing Company, 1974.
44. J.A. Havens, T.O. Spicer, *Development of an Atmospheric Dispersion Model for Heavier than Air GAs Mixtures*, Final Report to U.S. Coast Guard, CG-23-85, USCG HQ, Washington DC, 1985.
45. D.B. Turner, *Workbook of atmospheric dispersion estimate*. Environmental Protection Agency, Office of Air Programs Publication AP-26, Research Triangle Park, NC, 1970.
46. AIChE/CCPS, *Workbook of test cases for source characterisation and dispersion models for vapour clouds*, Center for Chemical Process Safety, AIChE, New York, 1989a.
47. J.S. Puttock, G.W. Colenbrander, D.R. Blackmore, *Field experiments on dense gas dispersion*, Jou. of Hazardous Materials 6, 1982.
48. R.P. Koopman, T.G. McRae, D.L. Goldwire, D.L. Ermak, E.J. Kansa, *Results of recent large-scale NH_3 and N_2O_4 dispersion experiments*, Heavy Gas and Risk Assessment III: Proc. of Third Sym. on Heavy Gases and Risk Assessment, Bonn Germany, 1984, distributed by Academic Press.
49. S. Andronopoulos, *A review of vapour cloud dispersion models*, Joint Research Centre - Ispra Site, EUR 14329 EN, 1992.
50. C.J.Wheatley, D.M. Webber, *Aspects of the dispersion of denser-than-air vapours relevant to gas cloud explosions*, Contract No. SR/007/80/UK/H, Report EUR 9592 EN, 1984.
51. R.J. Carpenter et al., *The Calculation of a Simple Model for dense gas dispersion using the Thorney Island, Phase I Data*, J.Haz.Mat., 16, pp.293-313.
52. D.M. Webber, C.J. Wheatley, *An Integral, Dynamic Turbulence Model for Heavy Gas Cloud Dispersal Close to the Source*, Report SRD R 437, 1987.
53. I.C. Ziomas et al., *Design of a System for Real-Time Modelling...*, J.Loss Prev. in the Proc.Ind., 2.
54. R.G. Picknett, *Field experiments on the behaviour of dense clouds*, Report Porton IL 1154/78/1.

55. G. Graziani et al., *Dispersione atmosferica di gas pesanti: sviluppo del modello MARA e suo confronto con dati sperimentali*, Report EUR 11132 IT, 1987.
56. L.S. Fryer, G.D. Kaiser, *DENZ, a computer program for the calculation of the dispersion of dense toxic or explosive gases in the atmosphere*, Report URAEA, SRD R 152, 1979.
57. S.F. Jagger, *Development of CRUNVCH: a dispersion model for continuous releases of denser-than-air vapour into the atmosphere*, Report UKAEA, SRD R229, 1983.
58. Canvey: *Summary of an investigation of potential hazards from operations in the Canvey Island/Thurrock Area*, HSE, Londra, 1982.
59. G.W. Colenbrander, *A mathematical model for the transient behaviour of dense vapour clouds*, 3rd Int.Sym. on Loss Prevention, Basel, Svizzera, 1980.
60. G.W. Colembrander, J.S. Puttock, IUTAM Symposium, Delft, Olanda, 1983.
61. J.A. Havens, T.O. Spicer, *Development of an Atmospheric dispersion model for heavier-than-air gas mixtures*, Rep.no. CG-D-22-85, FOR U.S. Coast Guard, Fayettville, 1985.
62. G. Spadoni et al., *A Model for the atmospheric dispersion of heavy gases*, Quad.Ing.Chim.Ital., Dicembre 1989.
63. S.R. Hanna, D.G. Stramaitis, J.H.Chang, *Hazardous Response Modeling Uncertainty (A Quantitative Method)*, Final Report - Vol.II, Sigma Research Corporation, April 1991.
64. M. Eltgroth, *Complex Hazard Air Release Model (CHARM) Version 6.0*, Technical document, Radian Corporation, Austin, TX 78720, 1990.
65. Quest Consultant Inc., *FOCUS*, 1988.
66. Cambridge Environmental Research Consultant, UK, and EnviroTech Research Ltd., Canada, *GASTAR 2.22*, 1988.
67. Technica Ltd., *PHAST 2.01*, 1991.
68. D.L. Ermak, *User's Manual for SLAB: An Atmospheric Dispersion Model for Denser-than-Air Releases (Draft, November Version)*, Lawrence Livermoore National Laboratory, Livermore, Ca 94550, 1989.
69. Ontario Ministry of the Environment (OME), *Portable Computing System for Use in Toxic Gas Emergencies*, Report No. ARB-162-83-ARSP, 1983.
70. R.N. Meroney, A. Lohmeyer, *Gravity Spreading and Dispersion of Dense GAs Clouds Released Suddenly into a Turbolent Boundary Layer*, Draft Report CER82-83RNM-A1-7 to GAs Research Institute, Chicago, IL, 1982.
71. V. Gudivaka, A. Kumar, *An Evaluation of four box Models for Istantaneous Dense-Gas Releases*, J of Hazardous MAterials, pp.237-255, 1990.
72. Thecnica Ltd., *WHAZAN*, 1990.
73. D.J. Finney, *Probit analysis*, 3rd edition, Cambridge University Press, 1971.
74. E.L. Anderson, *Quantitative approaches in use to assess cancer risk*, Risk Analysis 3(4), 1983.

75. *Methods for the determination of possible damage, CPR 16E,* TNO, Voorburg, The Netherlands, 1989.
76. W.E. Baker, P.A. Cox, P.S. Westine, J.J. Kulesz, R.A. Streholw, *Explosion hazards and evaluation,* Elsevier, New York, 1983.